Decadal forest soil organic matter pool responses to chronic manipulations of detrital input rates

by

Nicholas L. Medina

A thesis submitted in partial fulfillment
of the requirements for the degree of
Master of Science
(Ecology and Evolutionary Biology)
in the University of Michigan
2017

Master's Committee:

Professor Knute J. Nadelhoffer, Chair
Assistant Research Scientist Lucas E. Nave
Professor Donald R. Zak

To the unlabeled naturalists around the planet who deeply understand the value of soil organic matter in developing a healthy and sustainable relationship with our collective backyards, and continue to shape my eyes toward a moral code grounded in environmental sustainability

Table of contents

List of tables

List of figures

Abstract

Accurate descriptions of conceptual relationships between forest net primary productivity (NPP) and soil organic matter (SOM) dynamics remain important for reducing uncertainty in Earth system model projections. However, such descriptions ultimately depend on understanding of controls on long-term forest SOM pool dynamics, which remains incomplete. This is primarily because controls on detrital decay and soil respiration highlighted by many decomposition studies are rarely considered together with interactions with pre-existing SOM, which excludes potential feedbacks among SOM pools over decades of decomposition that shape net soil- and forest-atmosphere exchanges. This study describes potential dynamics among different temperate deciduous forest SOM pools underlying measured changes to total carbon (C), nitrogen (N), and natural ^{13}C and ^{15}N abundances of isolated A-horizon soil density fractions, as well as field rates of respired total C and ^{13}C from whole soil profiles. Results reveal the potential for non-linear decadal forest NPP-SOM relationships: chronic leaf and root exclusions resulted in net losses of total C and N, supporting positive forest NPP-SOM relationships. Chronic litter additions, however, resulted in no changes to total C and N, as well as faster incorporation of fresh particulate matter with high C:N ratios to aggregate-stabilized density fractions, suggesting increased turnover of stable SOM pools in response to more detrital inputs to soils. This may be due to N-limited decomposition, and a weaker forest NPP-SOM relationship than ecosystem models previously assume. Although stronger N limitation supports N-mining mechanisms that highlight the relevance of soil priming effects to net decadal forest SOM turnover, field soil respiration $\delta^{13}CO_2$ signatures suggest that any stable A-horizon SOM pools consist of fresh detritus, keeping A-horizon priming cryptic. However, field ^{13}C fluxes suggest strong contributions to soil C loss from deeper horizons, where the role of soil priming remains unclear

and SOM dynamics remain rarely quantified. Finally, my data suggested that temperature sensitivity may be another means by which detrital loading alters turnover. Ultimately, ecosystem model projections of land-atmosphere C feedbacks may be improved by considering additional factors likely to control long-term soil C turnover such as coarse soil texture and possible interactions with detrital production and soil temperature.

Introduction

Globally, soils release six times more carbon (C) annually to the atmosphere than do anthropogenic emissions, and contain more C as soil organic matter (SOM) than do plants and the atmosphere combined (Schlesinger and Bernhardt 2013), with residence times ranging from years to millennia (Torn et al. 1997). Earth system model (ESM) projections, however, have not converged on whether soils will be C sources or sinks in the coming decades (Hartmann et al. 2013). This is mainly due to limited understanding of long-term controls on SOM turnover (or stability) (Gottschalk et al. 2012; Bradford et al. 2016), despite that SOM turnover parameters have been suggested to be critical in reducing ecosystem model uncertainty (Keenan et al. 2013). Understanding long-term SOM turnover is especially important for determining the functioning of forests as the largest C sink on land (Pan et al. 2011), because SOM both releases greenhouse gases into the atmosphere and is an important source of nutrients needed for net primary productivity (NPP) (Schmidt et al. 2011).

Long-term controls on forest SOM turnover remain poorly understood in large part because rates of plant-derived detrital inputs to soils, including mainly sloughed root material, exudates, and leaf litter, are expected to change with NPP. NPP is expected to increase due to fertilization by rising atmospheric carbon dioxide (CO_2) levels (Norby et al. 2005; Schlesinger et al. 2006; De Kauwe et al. 2016), longer growing seasons (Linderholm 2006; Reyes-Fox et al. 2014), faster nutrient mineralization in warmer soils (Natali et al. 2014; Pold et al. 2015; Hicks Pries et al. 2016, 2017), and elevated atmospheric nitrogen (N) deposition (Nadelhoffer 2000; Hyvonen et al. 2007; Corre et al. 2010; Cusack et al. 2010, 2016; Li et al. 2015; Pisani et al. 2015; He et al. 2016). This is particularly true for temperate deciduous forests (Schlesinger et al. 2006; Springer and Thomas 2007; Ward et al. 2013), in which CO_2 fertilization has been linked

to higher NPP, greater forest floor accumulation (Schlesinger et al. 2006) and increased rates of detrital inputs to soils (White and Luo 2002; Bernhardt et al. 2006; Hoosbeek et al. 2006; Hasegawa et al. 2016). However, NPP could also decrease due to stronger water and nutrient limitations (Battipaglia et al. 2013; De Kauwe et al. 2013; Reich et al. 2014; van der Sleen et al. 2015; Wieder et al. 2015) and emerging plant pathogens (Smitley et al. 2008; Ramsfield et al. 2016).

Determinants of long-term forest SOM turnover are also poorly understood because most studies have focused on short-term (≤ 5-year) controls on SOM dynamics, which may not scale to describe SOM dynamics at decadal time scales across forest types (Foereid et al. 2014); although few studies have run long enough to test this (Lajtha et al. 2014; Pisani et al. 2016). Many previous studies of SOM dynamics highlight key physical and biochemical controls on detrital decomposition, such as initial biochemical properties (i.e. % N, % lignin, soluble phenolics, C:N ratios) (Berg 2014), soil temperature (Gregorich et al. 2016), and soil moisture and wet-dry cycle frequency (Kaiser et al. 2015). Results of these and other studies have led to ecosystem models in representing SOM accumulation primarily as a function of integrative detrital decay constants (often denoted as *k*); an approach that scales up to consider most forest NPP-SOM relationships as positive and linear (or first-order) at decadal-to-century time scales within individual climatic zones (Coleman and Jenkinson 1996).

However, especially at decadal scales, SOM accumulation is also affected by internal SOM dynamics, or interactions among pre-existing pools of SOM. Soil C models have incorporated separate SOM pools with distinct (Parton et al. 1987; Coleman and Jenkinson 1996) and calibrated turnover rates (Kamoni et al. 2007). However, few studies have run long enough to test hypotheses about SOM transfer among pools (Marin-Spiotta et al. 2009; Foote and

Grogan 2010; Plante et al. 2010; McFarlane et al. 2013; Bowden et al. 2014; Giardina et al. 2014; Lajtha et al. 2014; Mayzelle et al. 2014; Campo and Merino 2016; Pisani et al. 2016). Recent studies (Hatton et al. 2012; Lajtha et al. 2014; Cotrufo et al. 2015; Pisani et al. 2016) highlight a perspective on SOM pool turnover that focuses on factors affecting decomposer access to SOM, such as the strength and abundance of physical and chemical bonds between SOM and soil mineral particles (or organo-mineral complexes) (Dungait et al. 2012; Cotrufo et al. 2013; Lehmann and Kleber 2015). This perspective contrasts an older perspective that highlights common biochemical limits to decomposer activity, as measured by molecular weight and enzyme kinetics (Bosatta and Agren 1999; Veres et al. 2015). This continuum of mineral-SOM ratios integrates across biochemical controls on detrital decomposition and effects of longer-term soil properties such as structure and texture (Cotrufo et al. 2013; Kim et al. 2015; Rabbi et al. 2016), resulting in differences in soil density that have been interpreted as a viable correlates of SOM pool turnover (Crow et al. 2007). Such density fractionation procedures have been used to elucidate mechanisms mediating global change effects on long-term SOM turnover, helping to explain observed non-linearities in forest NPP-SOM relationships (Lajtha et al. 2014; Pisani et al. 2016).

Underlying causes of non-linear or even potentially negative forest NPP-SOM relationships also remain poorly understood. Decomposition studies have used natural abundance stable isotope mixing models to highlight controls on the magnitude of soil ‘priming effects’ as factors implicated in reducing total forest SOM stocks over time (Nottingham et al. 2012). Priming effects are originally defined as decreases in total SOM (increases in turnover) due to increased microbial activity and nutrient turnover resulting from labile inputs to soils (Brady and Weil 2008; Kuzyakov 2010), but have also refered to increases in total SOM (decreases in

turnover) in response to flushes of labile inputs ('positive' priming, compared to 'negative' priming) (Qiao et al. 2016). Mechanisms invoked for soil priming effects highlight key roles for passive SOM pools in contributing to increased SOM turnover (smaller stocks), such as in N-mining, in which passive, older SOM pools, often with lower C:N ratios compared to intact detritus, help alleviate strong N demands of microbial decomposers, induced by more C-rich inputs (Kuzyakov et al. 2000). In turn, evaluating total N and SOC can be used to indicate the magnitude and direction of priming in response to labile inputs, and ^{13}C and ^{15}N concentrations (especially of specific density fractions) can highlight potential mechanisms involved. Priming effects have been induced by a variety of sources of labile C inputs, including root exudates (Cheng 2011; Zhu et al. 2014), mycorrhizal fungi (Shahzad et al. 2015), and detrital inputs with varying C:N ratios (Qiao et al. 2016). Induction of SOM turnover rates by increased detrital input rates suggests that changes to forest NPP may induce soil priming effects, which in turn may cause forest NPP-SOM relationships to become neutral or negative, but few studies have tested this explicitly (Nottingham et al. 2012; Cardinael et al. 2015), while others imply its relevance in explaining spatial heterogeneity within forest soil C responses to global changes (Gottschalk et al. 2012). Results from Pisani et al. 2016 show that increases in aboveground litter production can result in lower net SOM stocks in fine-textured soils, although the role of decomposition processes implicated in priming remain unresolved. Furthermore, no studies have used density fractionation to highlight potential mechanisms proposed to explain priming effects, such as increased microbial activity and microbial N-mining (Chen et al. 2014), despite the potential for this method to help describe priming effects explicitly using internal SOM pool dynamics.

To better describe the potential effects of changing forest NPP on decadal SOM turnover and related mechanisms, my study used a subset of treated plots in a mid-successional temperate deciduous forest on a coarse-textured soil at the University of Michigan Biological Station (UMBS) in which detrital inputs (root and aboveground) were either excluded (No Input), detritus was left unmanipulated (Control), or leaf litter was experimentally doubled (Double Litter) for 10 years. To determine the general direction of net SOM turnover, total C and N stocks were quantified and considered with respect to their annual detrital input treatment. I predicted that C and N stocks would increase with detrital loading, assuming unchanging decomposition and SOM accretion rates per unit detrital input—this is consistent with representations of NPP-SOM dynamics in soil carbon models (Coleman and Jenkinson 1996) and does not assume priming effects. To further explain decadal SOM dynamics, in tandem with several studies that have analyzed SOM dynamics from the perspective of microbial access to SOM (McFarlane et al. 2013; Lajtha et al. 2014; Cotrufo et al. 2015; Hatton et al. 2015a), soils were fractionated by density (mass per unit particle volume) into three pools with varying mineral-SOM ratios and chemical compositions (Hatton et al. 2012; Moni et al. 2012). For this type of analysis, expected SOM pool turnover times have been presumed and shown to increase with fraction density in both fine- and coarse-textured soils (Crow et al. 2007, 2015; McFarlane et al. 2013). However, recent studies showing signatures of recently-incorporated SOM in denser fractions (Lajtha et al. 2014; Cotrufo et al. 2015; Hatton et al. 2015a) suggest that interpretations of density-based soil fractions alone, such as with modeled Δ^{14}C-based SOM turnover estimation, may not be entirely straightforward (Kleber et al. 2011). Nonetheless, I predicted that C and N concentrations would decrease with fraction density and increase with detrital loading, assuming that turnover times also increased with fraction density, and that turnover times did not

change over time nor in response to detrital manipulation—predictions further consistent with linear representations of NPP-SOM dynamics. Furthermore, to highlight potential SOM dynamics among fractions, natural ^{13}C and ^{15}N abundance ratios of each fraction were measured as an indication of the extent of SOM decay within the A horizon—inferences supported by natural abundance ^{13}C and ^{15}N soil depth profiles across horizons (Nadelhoffer and Fry 1988; Brunn et al. 2014). I hypothesized that the extent of decay, and thus ^{13}C and ^{15}N concentrations, would increase with both fraction density and detrital loading, assuming a unidirectional succession of SOM from labile and particulate to recalcitrant and mineral-sorbed, as well as no changes to turnover times with detrital manipulation. However, decreases in ^{13}C and ^{15}N concentrations with fraction density and/or detrital loading would suggest a possible role of soil priming effects in explaining decadal SOM turnover, with lower ^{15}N concentrations in a particular fraction indicating potentially dominant microbial N-mining mechanisms. To shed more light on SOM turnover, C mineralization rates were compared to pool sizes and sources using measurements of field CO_2 efflux rates—which have been shown to respond to long-term changes in forest floor accumulation (Bernhardt et al. 2006)—and natural ^{13}C abundances in respired CO_2, which taken together with ^{13}C depth profiles can indicate mineralization rates of older, more decomposed SOM. I hypothesized that the mineralization of older SOM, and thus $^{13}CO_2$ efflux, would not change with detrital loading, assuming turnover rates also did not change across treatments, which would result in net SOM accumulation with detrital loading. Finally, to highlight potential mediation of detrital loading effects on decadal SOM dynamics by soil temperature, field soil temperatures were measured at 5 cm depth; I hypothesized here that temperature variations would have separate, uniform effects on SOM responses to detrital manipulation.

Methods

Field site

This study was conducted at the University of Michigan Biological Station (UMBS), which is located on the south shore of Douglas Lake in Pellston, Michigan, USA (45°33.6' N and 84°42.6' W). The climate is temperate and is influenced by proximity to the Great Lakes: mean annual precipitation is 817 mm (including 294 mm as snow) and mean annual temperature is 5.5 ˚C. The forest is mixed deciduous and dominated by bigtooth aspen (*Populus grandidentata*), and secondarily by red maple (*Acer rubrum*), red oak (*Quercus rubra*), paper birch (*Betula papyrifera*), eastern white pine (*Pinus strobus*), sugar maple (*Acer saccharum*), American beech (*Fagus grandifolia*), and trembling aspen (*Populus tremuloides*). The detritus used for soil treatment reflected canopy overstory composition. Ground flora were systematically removed to normalize treatments and minimize heterogeneity in detritus input quality and quantity. Groundcover flora included *Gaultheria procumbens*, *Maianthemum canadense*, *Polygala paucifoia*, *Pteridium aquilinium*, and *Aralia nudicalus*. The forest has a history of both regular wildfire and human-induced fire, with an average return time of ~150 years in white pine and aspen dominated stands (Cleland et al. 2004), until it was extensively logged and burned until 1911, making the recovered overstory approximately 100 years old.

Soils are sandy Spodosols of the Rubicon series derived from glacial outwash, with O_i, O_e, A horizons ~5 cm deep and underlying E, B_s, and C horizon overlying >300 m of glacial deposits (sand and gravel). These soils are well-drained with low fertility, have 92% sand and 5% silt texture by weight, and pH values of 4.5 to 5.5 in water. Previous studies have quantified total N stocks up to 40 cm deep as 2,000 kg • ha^{-1}, an average N mineralization rate of 42 kg • ha^{-1} • yr^{-1} and < 2% net nitrification in these soils, along with 53% of fine-root biomass contained

within the top 30 cm (Nave et al. 2009). O_e and A horizons are also affected by regular European earthworm activity (Crumsey et al. 2013, 2014).

Experimental design

The UMBS DIRT site was established in 2004 and it belongs to an international network of long-term forest plant detrital manipulation plots called DIRT (Detrital Input and Removal Treatments) (Nadelhoffer et al. 2004). The site consists of 3 random blocks in areas with similar topography (≤ 100 m apart) that each contain nine 5x5 m plots: 1 plot per treatment per block. Each of the plots reported on in this study was re-treated annually for 10 years in the following manner: Control (C; non-manipulated litter and root inputs), Double Litter (DL; received 2 years' worth of leaf litter by combining captured plot litterfall and litterfall from detrital exclusion plots within the same block), and No Inputs (NI; both leaf litter removed and roots excluded with barriers up to 1 m). No Input plots were covered with rubber tarp whenever measurements were not being taken from them.

Soil sampling

Five subsamples were taken from the A-horizon of each plot using 10 cm x 10 cm sampling cores in October 2014 at random perpendicular distances across the diagonal of each plot. Samples were allowed to air-dry, passed through a 2-mm sieve, and corrected for moisture after oven-drying at 60˚C.

Sequential density fractionation

Equal masses (~10 g) of each plot's five subsamples were composited into a single bulk sample. Density fractionation was performed similar to that reported in (Crow et al. 2007) with the following exceptions: bulk soil was suspended in sodium polytungstate (SPT) (SPT-0, Geoliquids, Inc.) using a 2:1 soil-to-liquid volume ratio and centrifuged to separate SOM into three density fractions representing different SOM pools with different turnover times, mediated by variations in physical and chemical reactivity due to aggregation and organo-mineral complexation (Hatton et al. 2012): a free light fraction (fLF) composed mainly of coarse, loose particulate organic material, an intermediate fraction (IF) consisting of small macroaggregates (< 0.50 mm), and a dense fraction (DF) composed of organic matter bound tightly to soil mineral (mostly quartz sand) surfaces.

To first separate out the fLF from the combined IF and DF, the equivalent of ~20 g of oven-dry soil from the A horizon composites from each of the 3 replicate plots for each of Control, DL, and NI treatments (9 samples total, 3 per treatment, 1 per plot) was suspended in 50 mL SPT solution with a density of 1.85 ± 0.02 g • cm^{-3}. Later, a denser SPT solution of 2.40 ± 0.02 g • cm^{-3} was used to separate the remaining soil into an IF and DF fraction. The soil-SPT mixtures (soil from the first randomized block were analyzed first and done together) were shaken in 250-mL conical-tipped Nalgene centrifuge bottles on a bench-top shaker at 250 rpm for 2 h initially, and then for 10 min between attempts to collect the floating fLF and IF layers via aspiration. Centrifugation was performed using a Sorvall RT-H750 with no less than 900 x g for 1 h for the first separation (between fLF and IF) and 14 h for the second (between IF and DF). Stokes' Law was used to determine the appropriate centrifuge times to separate density fractions with a precision of ± 0.01 g • cm^{-3} at the target densities (1.85 and 2.40 g • cm^{-3}),

assuming that the dominant and smallest particle size in each fraction was 0.50 mm—representing small macroaggregates that were expected to be present in the IF—and 0.05 mm—representing fine sand in the DF. After the first round of centrifugation for each separation (first between the fLF and IF, and later between the IF and DF), the density of the SPT between the floating and denser layer was checked by filling and weighing a 5 mL volumetric flask, and adjustments were made as needed using either water or SPT solutions freshly mixed at higher or lower densities.

After collecting the fLF, residual SPT was removed via filtration with a Whatman GF/F filter and running 1 L of DI water through the collected layer. In contrast, residual SPT was removed from the collected IF and DF layers via re-suspension in 200 mL DI water and centrifugation for 10 min at first, and then subsequently 20 and 30 min. The IF and DF rinses were repeated 3 times until the density of the residual DI water in the bottle was ≤ 1.01 g • mL^{-1} These solutions were then discarded; the fLF leachates, however, were neutralized with 10% HCl for DOC and TDN measurement using a Shimadzu TOC-V_{SN} analyzer. All collected fractions were dried at 60˚C for at least 36 h and weighed.

A-horizon elemental and isotopic analysis

Each bulk soil and collected fraction was dried at 60 ˚C, subsampled for archiving, and ground using either a mortar and pestle or ball mill (Spex CertiPrep 8,000D-115). C and N concentrations were determined using oxidation-combustion with a CHN analyzer and balanced using the dry weight of each sample so that all fractions could be added and compared to bulk soil pools to determine total C and N recovered; ^{13}C and ^{15}N analyses were determined using isotope ratio mass spectrometry (IRMS) in the UMBS analytical chemistry laboratory.

Calculations of bulk mass, C and N stocks, and recovery of bulk C and N after density fractionation

Bulk C stocks were calculated by multiplying the density of solid soil mass (weight per volume of dry soil) by the concentration of C determined for bulk soils, and the same method was used to quantify bulk N stocks. To quantify total C present in each density fraction, the final oven-dry mass of the recovered fraction was divided by the mass of bulk soil used at the beginning of the fractionation process (~20 g) to determine the proportion of original bulk soil that the recovered fraction's mass represented, and this mass proportion was then multiplied by the bulk soil's average mass density at the plot level, as well as the percent C measured specifically for this recovered fraction mass. Finally, percent recovery of bulk C was determined by adding together by plot (one composite bulk soil sample was used per plot such that treatment $n = 3$) the total C present in each of the three density fractions, and subsequently dividing this sum by the mean plot-level bulk C stock; the same calculations were used to determine recovered bulk N and bulk mass density.

Field soil respiration measurements

Soil respiration rates were measured *in situ* using a LI-COR LI-6400 Portable Photosynthesis System that recorded CO_2 accumulation rates in soil surface enclosures. Each plot contained three 10 cm PVC collars that were inserted adjacent to each other along a single random side of the plot to approximately 12 cm depth at the start of every summer. For this study, soil respiration was measured from a pre-selected collar that most often showed median CO_2 efflux rates compared to the other two in the plot, so as to minimize the effects of within-plot

heterogeneity in respiration rates. Field respiration was measured this way for all treatments on three rain-free summer days in 2014: once each in July, August, and October. Field measurements took place between 10:00 and 19:30 EDT over a span of 5 to 8 hours. Up to 6 individual measurements were made on each collar, or fewer if concurrent readings varied by < 10%. Before averaging the readings, outliers that showed rates that differed by >10% of the other 5 readings were removed as a quality control precaution that minimizes the influence of machine reading error; this was rarely done. Individual CO_2 efflux rate readings were then averaged at the collar and treatment (across random blocks) levels for each month. One measurement of soil temperature at 5 cm depth was also made alongside respiration measurements using a thermocouple cable.

Field soil respiration $\delta^{13}CO_2$ and $^{13}CO_2$ efflux mass balance

Gas samples were extracted via syringes from the IRGA chambers used for flux measurements using immediately after respiration measurements were made. All samples were taken on the same day between 11:00 and 20:00 EDT. After equilibrating with ambient CO_2 concentrations, gas samples were taken using a Keeling-curve method (Pataki 2003): the IRGA chamber rested on a collar, and as the CO_2 concentration inside the chamber increased due to soil respiration, a syringe was used to extract 8 mL of gas from inside the IRGA chamber through its rubber septum. These samples were then transferred from syringes to 10-mL Helium-flushed vials. This extraction was repeated 5 times over regular intervals (≥40 ppm increases in CO_2 concentrations) for each collar for a total of 5 gas samples per collar. Collected gas was analyzed using IRMS, and the $\delta^{13}CO_2$ values of these 5 samples were then regressed as function of inverse CO_2 concentration ($[CO_2]^{-1}$) and the intercept was used as the concentration-independent

$\delta^{13}CO_2$ value for soil respiration from the plot. The $^{13}CO_2$ efflux rates were calculated using VPDB and VPD standard ratios to yield $^{13}C/^{12}C$ atom percent values that were then multiplied by the total plot-level CO_2 efflux measurement means.

Statistical analysis

RStudio version 1.0.136 was used to perform analyses of variance (ANOVA) or general linear model (GLM) regressions on *in situ* field soil respiration rates, $\delta^{13}CO_2$ signatures of respired carbon, field temperatures, and A-horizon C, N, ^{13}C, and ^{15}N data. After evaluating a general treatment effect, Tukey HSD or Dunnet-type (comparisons only with Control) linear mixed effects (LME) models were used as post-hoc tests to account for unbalanced measurement inputs and to eliminate block-level pairwise comparisons for CO_2 effluxes and $\delta^{13}CO_2$ values with the probability of making a type I error, $\alpha = 0.05$. These statistical tests were performed using the 'multcomp', 'lme4', 'dplyr', and 'reshape2' packages, and figures were made using either Microsoft Excel version 15.33 or in RStudio (1.0.136) also using the 'ggplot2', 'grid', and 'gridExtra' packages.

Results

Recovery of bulk soils by sequential density fractionation

A decade of leaf and root exclusions (No Input, NI) resulted in lower bulk C ($p < 0.05$) and N ($p < 0.001$) stocks compared to the Control treatment, whereas leaf litter additions (Double Litter, DL) resulted in no changes to bulk C and N stocks (Table 1, Fig 1). Such detrital manipulation affects bulk C and N stocks more strongly than did the relative contributions of random block effects on bulk mass densities (Table 1). Of bulk soils, mass recovery was near complete and independent of treatment, and the majority (approximately three-fourths) of bulk soil mass was represented by the densest soil fraction. However, the recovery of bulk C (70%) and N (50%) was limited to the total C and N stock of the No Input treatment, resulting in less total recovered C and N in Control and Double Litter treatments compared their stocks as calculated using bulk C and N concentrations (Table 2). Despite this, C and N stock sizes of Double Litter treatments compared similarly to those of Control when calculated using bulk soil C and N concentrations as when calculated using combined density fraction concentrations (Table 1, Fig 1). Furthermore, differences in both bulk soil mass and recovered masses of all three density fractions were explained in part by random block effects (Table 2). In all treatments, most (approximately two-thirds of recovered) C and N was present as unprotected particulate matter, and this light particulate fraction yielded leachates that showed decreasing in DOC and TDN concentration with detrital loading (Table 1).

Density fraction chemistry

The lightest fraction (free light fraction, fLF) was defined as all soil content less than 1.85 g • cm^{-3}, and indicates SOM in particulate form, making it relatively labile and unstable compared to

other SOM fractions (Crow et al. 2007). In these soils, C and N stocks decreased with fraction density, highlighting that most SOM (approximately two-thirds) was present in this form (Table 1, Fig 1). The intermediate fraction (IF), defined by all soil content between 1.85 and 2.4 g • cm^{-3}, was targeted to isolate mainly small macroaggregates (< 0.50 mm) and represent SOM that is presumably less accessible to microbial degradation compared to the free-light fraction, but more so than than tightly-bound mineral-sorbed SOM in the dense fraction. Intermediate fraction C:N ratios showed an increasing trend with detrital loading, while C and N concentrations varied minimally by random block (Table 1). Specifically, the C:N ratio of soils with added litter was 25% higher than that of soils without detritus (Appendix) and did not differ from that of Control soils. The dense fraction, defined as all soil content denser than 2.4 g • cm^{-3}, usually represents SOM that is most tightly bound to primary and secondary mineral surfaces, and therefore the least susceptible to microbial mineralization. While the range of dense fraction C:N ratios was wide among treated soils, large variation in No Input soils limited the detection of statistically significant differences, despite the likelihood of observing them with repeated sampling and/or larger sample sizes. In all soils, C and N concentrations and stocks increased with fraction density (Table 1, Fig 1). However, Double Litter soils were unique in showing higher C:N ratios with increasing fraction density (Table 1).

Field soil respiration rates

Throughout the season, field soil CO_2 efflux rates tended to increase with chronic detritus loading (Fig 2). In July, soil CO_2 effluxes differed among experimental treatments: DL soils released CO_2 37% faster (Appendix) than did Control soils. Also in July, NI soils released CO_2 42% slower (Appendix) than Control soils. In August, DL soils respired 45% faster than Control

soils by (Appendix), and NI soils appeared ($p > 0.05$) to respire slower than Control soils. In October, CO_2 efflux rates were lower overall, but a weak (non-significant) trend of increasing CO_2 efflux with increased detrital loading across treatments was present in the data.

Field soil respiration $\delta^{13}CO_2$

Patterns in differences among mean respired $\delta^{13}CO_2$ values in response to chronic detrital manipulation were opposite to those that emerged from field soil CO_2 efflux rate measurements, as discussed above (Fig 2). Throughout the season, $\delta^{13}CO_2$ values of soil respiration from all treatments were higher than $\delta^{13}C$ values recorded for intact leaf litter of the O_i horizon at this site (Vogel, unpublished data). In July, DL $\delta^{13}CO_2$ were much lower ($p < 0.001$) lower than those of Control soils, by 2.6‰ (Fig 3), and were again lower than Control in August by 1.5‰ (Fig 3). Throughout the season, NI $\delta^{13}CO_2$ values did not differ from those of Control soils. By October, DL $\delta^{13}CO_2$ values increased enough to match Control and NI soil respiration $\delta^{13}CO_2$ value ranges, showing the convergence of $\delta^{13}CO_2$ values across all treatments through the season. Throughout the season, NI $\delta^{13}CO_2$ values were consistently not different from those of Control. Overall, a significantly negative correlation (*slope* = -0.28273) emerged between total field soil CO_2 efflux rate and $\delta^{13}CO_2$ values of field soil respiration, such that total CO_2 efflux rate explained 39% of the variation in $\delta^{13}CO_2$ values (Fig S1).

While mean DL soil respiration $\delta^{13}CO_2$ values were lower compared to those from Control soils, total mass-balanced $^{13}CO_2$ efflux rates followed trends in total CO_2 efflux rates (Fig S2). Specifically, mean $^{13}CO_2$ efflux rates from DL soils were higher than from Control soils by 37% in July, and 45% (Appendix) in August. In July, NI soils were lower than Control rates by 42%

(Appendix). October mean $^{13}CO_2$ efflux rates were lower overall, and showed a weak (non-significant) trend of increasing $^{13}CO_2$ efflux with increasing litter loading across treatments.

A-horizon field soil temperatures

Mean field soil temperatures were measured to evaluate their role in explaining CO_2 effluxes. Mean soil temperatures were not different across treatments (Table S1) during all three months (Fig S3), and were lower in October (Appendix). These temperature drops in October also highlighted a very significant ($p < 0.01$) temperature-by-treatment interaction (Appendix) that affected both total soil CO_2 efflux rates and mass-balanced $^{13}CO_2$ efflux rates (Fig S4), such that warmer soils that received more detrital inputs annually also released both total CO_2 and $^{13}CO_2$ faster. At higher mean soil temperatures, mean DL respiration rates were higher than Control rates, which were in turn higher than those of NI (Appendix). At lower mean soil temperatures, CO_2 and CO_2 efflux rates were similar across treatments.

Discussion

Initially, I hypothesized that detrital loading would not point to changes in SOM turnover—in accord with previous ecosystem model assumptions about linear, positive, and robust relationships between total annual forest NPP and total SOM pool sizes (Coleman and Jenkinson 1996; Gottschalk et al. 2012)—thereby predicting observations of increased C and N concentrations, stocks, and natural ^{13}C and ^{15}N abundances with detrital loading. Surprisingly, this was only partially supported by the collection of data presented here. In the case that factors like mineral-SOM ratios and microbial C-use efficiency do not change, manipulated input rates to soils would be expected to result in parallel changes to SOM stock size. In the case of detrital exclusion, decreases in SOM stock size were indeed observed, suggesting minimal to no changes in SOM turnover rate.

However, in the case of chronic litter additions, SOM stock data did not support proposed predictions and hypotheses related to unchanging turnover. Double Litter soils showed no increases in SOM stock size, but did show increases in soil respiration (representing C loss from soil). Such an increase in respired C without an increase in accumulated C suggests a potential overall decrease in C-use efficiency of decomposer communities, indicating a mechanism by which detrital loading may induce changes to overall SOM turnover. In addition to these trends in field soil respiration, relatively high C:N ratios of the Double Litter treatment suggest that although the A-horizon SOM pool is receiving twice the background (control) rates of above-ground litter input, it is not increasing detectably in size. This results in increased turnover rates of all three A-horizon SOM pools in the coarse-textured soil of this temperate mid-successional deciduous forest, and possibly also suggest increasing N limitation for decomposer activity and plant growth with detrital loading.

However, my interpretation is limited by an effect of detrital manipulation on the ability of sequential density fractionation to recover free light fraction C and N. While most C and N was present in loose particulate form in this coarse-textured soil, the free light fraction was also most sensitive to loss during suspension in SPT given that it represented the least mass compared to the two other soil fractions. Additionally, some differences in recovery could be explained by random spatial block (Table 1,2), which, given the presence of such block effects in bulk mass density, C, and N stocks, may indicate sensitivity of C and N stocks to minor site heterogeneity within this forest. This fraction's relative contribution to total C and N, as well as its chemical properties, showed no response to detrital manipulation, suggesting that such changes may not be controlled by detrital input rate, but instead potentially by detrital quality. Recent work by Hatton et al 2015 suggests that root detritus is more likely than leaf litter to persist in soils as particulate matter. Particulate N concentrations could also be controlled by small but long-term site variation, as suggested by small but significant differences in fLF N concentrations among random blocks for all treatments (Table 1). However, such changes in N were not enough to cause changes in particulate C:N ratios among treatments, and therefore perhaps did not affect SOM dynamics. Finally, while the mean soil respiration rate from the Double Litter treatment plus the collected soil leachates did not account for enough C to balance the extra leaf inputs added annually, these data still may suggest a potential increase in turnover rate of part of the total SOM, particularly if the material not accounted for ultimately gets transferred to lower soil horizons.

While little quantitative data is currently available on the rates of SOM transfer among soil horizons, deeper soil horizons are likely to play a role in mediating changing forest NPP and detrital input rates on net forest SOM turnover. In this study, because detrital addition treatments

input more organic material than was accounted for in A horizon SOM, some SOM may have been transferred to E and/or B_s horizons either by leaching *in situ* or fungal hyphae. Such transfer is likely if the A horizon at this site is saturated, which is possible given low mineral surface area available for organo-mineral complexation compared to finer-textured soils where SOM accretion in response to detrital addition has been observed (Lajtha et al. 2014). It should be noted that SOM stasis has also been observed at loamy sites (Pisani et al. 2016). At this site, the soil fraction considered here with the most support for altered turnover is that which slightly resembled lower horizons—the intermediate fraction (with high physicochemical occlusion)—pointing toward a possible role of mineral and/or texture-dependent factors in altering the turnover of A-horizon SOM. That the mineral-rich and presumably most stable SOM pool was quickest to respond with potential changes in turnover was surprising, given that two-thirds of all SOM was present in particulate form in these soils; such a large proportion of particulate SOM is expected to make up much of the SOM at this site susceptible to mineralization and microbial transformation. Ultimately, however, higher overall turnover was suggested for the aggregated fraction by significantly higher C:N ratios in the soil fraction with intermediate density in response to added litter. This result suggests that detrital effects on SOM turnover may be mediated by the predominance of aggregation and soil structure in general, which is in turn in part determined by soil forming factors such as parent material, climate, plant roots, and microbial activity. In accordance with recent analyses, this may highlight the importance of interactions among soil state factors in mediating global change effects on long-term forest SOM turnover. Additionally, McFarlane et al 2013 observed that coarse-textured soil profiles similar to those at this site store relatively little C compared to sites even nearby with finer textures. At the same time, such soils with lower total C stocks also contain C that is distributed more evenly

among 15-cm depths up to 90 cm. This compares to those sites with finer textures and larger total C stocks, which increasingly store more C in horizons below the A within 5-30 cm. Given that all sites in their study had similar A horizon C content regardless of detrital input rates, and that similar results for this horizon were observed in this study, there is support in considering forest A horizon SOM stocks as a whole to turn over very quickly. As a result, future forest SOM studies could consider evaluating deep soil C dynamics in response to long-term treatments.

The rapid response in turnover change observed here for the densest fraction compared to lighter fractions provides evidence against the use of physical stability (density fractions, or degree of organo-mineral association) in defining SOM pools with distinct turnover rates. On the other hand, the quick incorporation of leaf litter-derived detritus into mineral- and aggregate-stable SOM pools has also been observed in other studies (Cotrufo et al. 2015; Hatton et al. 2015b), but has not been widely suggested as a potential driver of changes in SOM turnover. To result in a change in turnover, processes involved in the physical and chemical destabilization of SOM would have to play a large role in making fresh litter available again to decomposers after mineral sorption, but few studies have tested the importance of this (Keiluweit et al. 2015). Mechanisms implicated in soil priming such as root exudation and N mining by decomposers to meet stoichiometric C:N demands (Kuzyakov 2010) have the potential to control changes to decadal SOM turnover, but their importance has rarely been tested (Cardinael et al. 2015).

Results presented here are inconclusive with regard to priming-related mechanisms. Natural $^{13}CO_2$ abundances in field soil respiration were measured to highlight the contribution of old and stable SOM to most soil C mineralization. If priming were a key process shaping detritus-induced C fluxes, respired ^{13}C concentration would be expected to increase with detrital loading, based on interpretations of isotopic depth profiles (Nadelhoffer and Fry 1988). Instead, a

trend of proportionally less respired ^{13}C was found with detrital loading, which, while not what was predicted, may also not strictly rule out priming mechanisms. Recent work by Hatton et al 2015 and Cotrufo et al 2015 used isotopic data to infer that labile C from recently-decomposed detritus is very quickly stabilized via sorption to soil mineral particles, which implies that some pools of physically stabilized SOM may contain very low ^{13}C concentrations, making accelerated turnover of such pools difficult to detect using field soil respiration measurements, perhaps due to particulate A-horizon SOM and forest floor accumulation that is proportionally rich in ^{12}C. Given that the intermediate fraction, richest in ^{13}C, still had concentrations lower than those of field soil respiration, large contributions of respiration from lower in the soil profile are likely. However, isotopic data presented here suggest the release of more recent detrital inputs from soils subject to more detrital inputs. As a result, priming may help explain potentially higher turnover in the A horizon, but future studies may need to be detected using additional techniques. However, increases in C:N ratios with litter loading and with fraction density in Double Litter soils may have been caused by slight decreases in N concentration, which would support the microbial demand for N as a reason for the lack of SOM accumulation in response to litter additions.

Another mechanism potentially explaining higher turnover in response to litter additions is an increase in temperature sensitivity of SOM pools, which was not hypothesized to be involved. I predicted that detrital inputs would not mediate a response of density fractions to temperature sensitivity, as per kinetic theory, which predicts lower temperature sensitivity for more stable SOM pools because temperature cannot change biochemical barriers to enzyme activity (Bosatta and Agren 1999). However, recent findings that fresh detritus is the primary source for stable SOM pools suggest that (Lajtha et al. 2014; Hatton et al. 2015b), coupled with

mineral dissociation mechanisms such as root exudation, stable SOM pools should be more temperature sensitive. Results here support that more physically stable SOM pools, as measured by denser fractions, are more temperature sensitive, via a clear temperature-by-treatment interaction explaining field soil respiration rates as a function of A horizon field soil temperature (Fig S4).

Overall, my study highlights the potential for non-linear relationships between NPP and SOM accumulation in temperate deciduous forests via potential turnover rate changes for the most stable of SOM pools. This is supported by a lack of increases in SOM stocks as well as higher C:N ratios in aggregate-stabilized soil fractions. This finding further highlights the importance of detrital inputs rates to soils in determining SOM turnover rates, which is expected to feed back both directly to atmospheric warming in the coming decades, as well as indirectly via effects on long-term forest growth.

References

Battipaglia G, Saurer M, Cherubini P, et al (2013) Elevated CO2 increases tree-level intrinsic water use efficiency: Insights from carbon and oxygen isotope analyses in tree rings across three forest FACE sites. New Phytol 197:544–554. doi: 10.1111/nph.12044

Berg B (2014) Decomposition patterns for foliar litter - A theory for influencing factors. Soil Biol Biochem 78:222–232. doi: 10.1016/j.soilbio.2014.08.005

Bernhardt ES, Barber JJ, Pippen JS, et al (2006) Long-term effects of free air CO2 enrichment (FACE) on soil respiration. Biogeochemistry 77:91–116. doi: 10.1007/s10533-005-1062-0

Bosatta E, Agren GI (1999) Soil organic matter quality interpreted thermodynamically. Soil Biol Biochem 31:1889–1891. doi: 10.1016/s0038-0717(99)00105-4

Bowden RD, Deem L, Plante AF, et al (2014) Litter Input Controls on Soil Carbon in a Temperate Deciduous Forest. North Am For Soils S66–S75. doi: 10.2136/sssaj2013.09.0413nafsc

Bradford MA, Bonan GB, Noah Fierer, Peter A. Raymond, & Thomas W. Crowther WRW (2016) Managing uncertainty in soil carbon feedbacks to climate change.

Brady NC, Weil RR (2008) The nature and properties of soils. Macmillan Publ CoNew York 13:960.

Brunn M, Spielvogel S, Sauer T, Oelmann Y (2014) Temperature and precipitation effects on δ13C depth profiles in SOM under temperate beech forests. Geoderma 235–236:146–153. doi: 10.1016/j.geoderma.2014.07.007

Campo J, Merino A (2016) Variations in soil carbon sequestration and their determinants along a precipitation gradient in seasonally dry tropical forest ecosystems. Glob Chang Biol 22:1942–1956. doi: 10.1111/gcb.13244

Cardinael R, Eglin T, Guenet B, et al (2015) Is priming effect a significant process for long-term SOC dynamics? Analysis of a 52-years old experiment. Biogeochemistry 123:203–219. doi: 10.1007/s10533-014-0063-2

Chen R, Senbayram M, Blagodatsky S, et al (2014) Soil C and N availability determine the priming effect: Microbial N mining and stoichiometric decomposition theories. Glob Chang Biol. doi: 10.1111/gcb.12475

Cheng Z and (2011) Rhizosphere priming effect increases the temperature sensitivity of soil organic matter decomposition.

Cleland DT, Crow TR, Saunders SC, et al (2004) Characterizing historical and modern fire regimes in Michigan (USA): A landscape ecosystem approach. In: Landscape Ecology. pp 311–325

Coleman K, Jenkinson D. (1996) RothC - A Model for the Turnover of Carbon in Soil. In: Evaluation of Soil Organic Matter Models: Using Existing Long-Term Datasets. pp 237–246

Corre MD, Veldkamp E, Arnold J, Joseph Wright S (2010) Impact of elevated N input on soil N cycling and losses in old-growth lowland and montane forests in Panama. Ecology 91:1715–1729. doi: 10.1890/09-0274.1

Cotrufo MF, Horton AJ, Campbell EE, et al (2015) Formation of soil organic matter via biochemical and physical pathways of litter mass loss. Nat Geosci 8:776–781.

Cotrufo MF, Wallenstein MD, Boot CM, et al (2013) The Microbial Efficiency-Matrix Stabilization (MEMS) framework integrates plant litter decomposition with soil organic matter stabilization: Do labile plant inputs form stable soil organic matter? Glob Chang Biol 19:988–995. doi: 10.1111/gcb.12113

Crow SE, Reeves M, Schubert OS, Sierra CA (2015) Optimization of method to quantify soil organic matter dynamics and carbon sequestration potential in volcanic ash soils. Biogeochemistry 123:27–47. doi: 10.1007/s10533-014-0051-6

Crow SE, Swanston CW, Lajtha K, et al (2007) Density fractionation of forest soils: Methodological questions and interpretation of incubation results and turnover time in an ecosystem context. Biogeochemistry 85:69–90. doi: 10.1007/s10533-007-9100-8

Crumsey JM, Le Moine JM, Capowiez Y, et al (2013) Community-specific impacts of exotic earthworm invasions on soil carbon dynamics in a sandy temperate forest. Ecology 94:2827–2837. doi: 10.1890/12-1555.1

Crumsey JM, Le Moine JM, Vogel CS, Nadelhoffer KJ (2014) Historical patterns of exotic earthworm distributions inform contemporary associations with soil physical and chemical factors across a northern temperate forest. Soil Biol Biochem 68:503–514. doi: 10.1016/j.soilbio.2013.10.029

Cusack DF, Macy J, McDowell WH (2016) Nitrogen additions mobilize soil base cations in two tropical forests. Biogeochemistry 128:67–88. doi: 10.1007/s10533-016-0195-7

Cusack DF, Torn MS, Mcdowell WH, Silver WL (2010) The response of heterotrophic activity and carbon cycling to nitrogen additions and warming in two tropical soils. Glob Chang Biol 16:2555–2572. doi: 10.1111/j.1365-2486.2009.02131.x

De Kauwe MG, Keenan TF, Medlyn BE, et al (2016) Satellite based estimates underestimate the effect of CO2 fertilization on net primary productivity. Nat Clim Chang 6:892–893. doi: 10.1038/nclimate3105

De Kauwe MG, Medlyn BE, Zaehle S, et al (2013) Forest water use and water use efficiency at elevated CO2: A model-data intercomparison at two contrasting temperate forest FACE

sites. Glob Chang Biol 19:1759–1779. doi: 10.1111/gcb.12164

Dungait JAJ, Hopkins DW, Gregory AS, Whitmore AP (2012) Soil organic matter turnover is governed by accessibility not recalcitrance. Glob Chang Biol 18:1781–1796. doi: 10.1111/j.1365-2486.2012.02665.x

Foereid B, Ward DS, Mahowald N, et al (2014) The sensitivity of carbon turnover in the community land model to modified assumptions about soil processes. Earth Syst Dyn 5:211–221. doi: 10.5194/esd-5-211-2014

Foote RL, Grogan P (2010) Soil carbon accumulation during temperate forest succession on abandoned low productivity agricultural lands. Ecosystems 13:795–812. doi: 10.1007/s10021-010-9355-0

Giardina CP, Litton CM, Crow SE, Asner GP (2014) Warming-related increases in soil CO2 efflux are explained by increased below-ground carbon flux. Nat Clim Chang 4:822–827. doi: 10.1038/NCLIMATE2322

Gottschalk P, Smith JU, Wattenbach M, et al (2012) How will organic carbon stocks in mineral soils evolve under future climate? Global projections using RothC for a range of climate change scenarios. Biogeosciences 9:3151–3171. doi: 10.5194/bg-9-3151-2012

Gregorich EG, Janzen H, Ellert BH, et al (2016) Litter decay controlled by temperature, not soil properties, affecting future soil carbon. Glob Chang Biol. doi: 10.1111/gcb.13502

Hartmann DL, Tank AMGK, Rusticucci M (2013) IPCC Fifth Assessment Report, Climate Change 2013: The Physical Science Basis. IPCC AR5:31–39.

Hasegawa S, Macdonald CA, Power SA (2016) Elevated carbon dioxide increases soil nitrogen and phosphorus availability in a phosphorus-limited Eucalyptus woodland. Glob Chang Biol 22:1628–1643. doi: 10.1111/gcb.13147

Hatton P-J, Castanha C, Torn MS, Bird JA (2015a) Litter type control on soil C and N stabilization dynamics in a temperate forest. Glob Chang Biol 1358–1367. doi: 10.1111/gcb.12786

Hatton PJ, Castanha C, Torn MS, Bird JA (2015b) Litter type control on soil C and N stabilization dynamics in a temperate forest. Glob Chang Biol 21:1358–1367. doi: 10.1111/gcb.12786

Hatton PJ, Kleber M, Zeller B, et al (2012) Transfer of litter-derived N to soil mineral-organic associations: Evidence from decadal 15N tracer experiments. Org Geochem 42:1489–1501. doi: 10.1016/j.orggeochem.2011.05.002

He K, Qi Y, Huang Y, et al (2016) Response of aboveground biomass and diversity to nitrogen addition – a five-year experiment in semi-arid grassland of Inner Mongolia, China. Sci Rep 6:31919. doi: 10.1038/srep31919

Hicks Pries CE, Castanha C, Porras R, Torn MS (2017) The whole-soil carbon flux in response to warming. Science (80-) 1319:eaal1319. doi: 10.1126/science.aal1319

Hicks Pries CE, Schuur EAG, Natali SM, Crummer KG (2016) Old soil carbon losses increase with ecosystem respiration in experimentally thawed tundra. Nat Clim Chang 6:214–218. doi: 10.1038/nclimate2830

Hoosbeek MR, Li Y, Scarascia-Mugnozza GE (2006) Free atmospheric CO2 enrichment (FACE) increased labile and total carbon in the mineral soil of a short rotation Poplar plantation. Plant Soil 281:247–254. doi: 10.1007/s11104-005-4293-x

Hyvonen R, Agren GI, Linder S, et al (2007) The likely impact of elevated [CO2], nitrogen deposition, increased temperature and management on carbon sequestration in temperate and boreal forest ecosystems: a literature review. New Phytol 173:463–480. doi:

10.1111/j.1469-8137.2007.01967.x

Kaiser M, Kleber M, Berhe AA (2015) How air-drying and rewetting modify soil organic matter characteristics: An assessment to improve data interpretation and inference. Soil Biol Biochem 80:324–340. doi: 10.1016/j.soilbio.2014.10.018

Kamoni PT, Gicheru PT, Wokabi SM, et al (2007) Predicted soil organic carbon stocks and changes in Kenya between 1990 and 2030. Agric Ecosyst Environ 122:105–113. doi: 10.1016/j.agee.2007.01.024

Keenan TF, Davidson E a., Munger JW, Richardson AD (2013) Rate my data: quantifying the value of ecological data for the development of models of the terrestrial carbon cycle. Ecol Appl 23:273–86. doi: 10.1890/12-0747.1

Keiluweit M, Nico PS, Pett-Ridge J, et al (2015) Mineral protection of soil carbon counteracted by root exudates. Nat Clim Chang 5:588–595.

Kim H, Nunan N, Dechesne A, et al (2015) The spatial distribution of exoenzyme activities across the soil micro-landscape, as measured in micro- and macro-aggregates, and ecosystem processes. Soil Biol Biochem 91:258–267. doi: 10.1016/j.soilbio.2015.08.042

Kleber M, Nico PS, Plante A, et al (2011) Old and stable soil organic matter is not necessarily chemically recalcitrant: Implications for modeling concepts and temperature sensitivity. Glob Chang Biol 17:1097–1107. doi: 10.1111/j.1365-2486.2010.02278.x

Kuzyakov Y (2010) Priming effects: Interactions between living and dead organic matter. Soil Biol Biochem 42:1363–1371. doi: 10.1016/j.soilbio.2010.04.003

Kuzyakov Y, Friedel JK, Stahr K (2000) Review of mechanisms and quantification of priming effects. Soil Biol Biochem 32:1485–1498. doi: 10.1016/S0038-0717(00)00084-5

Lajtha K, Townsend KL, Kramer MG, et al (2014) Changes to particulate versus mineral-

associated soil carbon after 50 years of litter manipulation in forest and prairie experimental ecosystems. Biogeochemistry 119:341–360. doi: 10.1007/s10533-014-9970-5

Lehmann J, Kleber M (2015) The contentious nature of soil organic matter. Nature 528:60–8. doi: 10.1038/nature16069

Li W, Jin C, Guan D, et al (2015) The effects of simulated nitrogen deposition on plant root traits: A meta-analysis. Soil Biol Biochem 82:112–118. doi: 10.1016/j.soilbio.2015.01.001

Linderholm HW (2006) Growing season changes in the last century. Agric For Meteorol 137:1–14.

Marin-Spiotta E, Silver WL, Swanston CW, Ostertag R (2009) Soil organic matter dynamics during 80 years of reforestation of tropical pastures. Glob Chang Biol 15:1584–1597. doi: 10.1111/j.1365-2486.2008.01805.x

Mayzelle MM, Krusor ML, Lajtha K, et al (2014) Effects of Detrital Inputs and Roots on Carbon Saturation Deficit of a Temperate Forest Soil. Soil Sci Soc Am J 78:S76. doi: 10.2136/sssaj2013.09.0415nafsc

McFarlane KJ, Torn MS, Hanson PJ, et al (2013) Comparison of soil organic matter dynamics at five temperate deciduous forests with physical fractionation and radiocarbon measurements. Biogeochemistry 112:457–476. doi: 10.1007/s10533-012-9740-1

Moni C, Derrien D, Hatton PJ, et al (2012) Density fractions versus size separates: Does physical fractionation isolate functional soil compartments? Biogeosciences 9:5181–5197. doi: 10.5194/bg-9-5181-2012

Nadelhoffer KJ (2000) The potential effects of nitrogen deposition on fine-root production in forest ecosystems. New Phytol 147:131–139. doi: 10.1046/j.1469-8137.2000.00677.x

Nadelhoffer KJ, Boone RD, Bowden RD, et al (2004) The DIRT Experiment: Litter and Root

Influences on Forest Soil Organic Matter Stocks and Function. For time Environ consequences 1000 years Chang New Engl 300–315.

Nadelhoffer KJ, Fry B (1988) Controls on Natural Nitrogen-15 and Carbon-13 Abundances in Forest Soil Organic Matter. Soil Sci Soc Am J 52:1633. doi: 10.2136/sssaj1988.03615995005200060024x

Natali SM, Schuur EAG, Webb EE, et al (2014) Permafrost degradation stimulates carbon loss from experimentally warmed tundra. Ecology 95:602–608. doi: 10.1890/13-0602.1

Nave LE, Swanston CW, Curtis PS, Vance ED (2009) Impacts of elevated inputs on north temperate forest soil C storage, C/N, and net N-mineralization. Geoderma 153:231–240.

Norby RJ, DeLucia EH, Gielen B, et al (2005) Forest response to elevated CO2 is conserved across a broad range of productivity. Proc Natl Acad Sci 102:18052–18056. doi: 10.1073/pnas.0509478102

Nottingham AT, Turner BL, Chamberlain PM, et al (2012) Priming and microbial nutrient limitation in lowland tropical forest soils of contrasting fertility. Biogeochemistry 111:219–237. doi: 10.1007/s10533-011-9637-4

Pan Y, Birdsey R a, Fang J, et al (2011) A Large and Persistent Carbon Sink in the World's Forests. Sciencexpress 14:1–11. doi: 10.1126/science.1201609

Parton WJ, Schimel DS, Cole C V, Ojima DS (1987) Analysis of Factors Controlling Soil Organic Matter Levels in Great Plains Grasslands. Soil Sci Soc Am J 51:1173–1179. doi: 10.2136/sssaj1987.03615995005100050015x

Pisani O, Frey SD, Simpson AJ, Simpson MJ (2015) Soil warming and nitrogen deposition alter soil organic matter composition at the molecular-level. Biogeochemistry 123:391–409. doi: 10.1007/s10533-015-0073-8

Pisani O, Lin LH, Lun OOY, et al (2016) Long-term doubling of litter inputs accelerates soil organic matter degradation and reduces soil carbon stocks. Biogeochemistry 127:1–14.

Plante AF, Conant RT, Carlson J, et al (2010) Decomposition temperature sensitivity of isolated soil organic matter fractions. Soil Biol Biochem 42:1991–1996. doi: 10.1016/j.soilbio.2010.07.022

Pold G, Melillo JM, DeAngelis KM (2015) Two decades of warming increases diversity of a potentially lignolytic bacterial community. Front Microbiol. doi: 10.3389/fmicb.2015.00480

Qiao N, Xu X, Hu Y, et al (2016) Carbon and nitrogen additions induce distinct priming effects along an organic-matter decay continuum. Sci Rep 6:19865. doi: 10.1038/srep19865

Rabbi SMF, Daniel H, Lockwood P V., et al (2016) Physical soil architectural traits are functionally linked to carbon decomposition and bacterial diversity. Sci Rep 6:33012. doi: 10.1038/srep33012

Ramsfield TD, Bentz BJ, Faccoli M, et al (2016) Forest health in a changing world: Effects of globalization and climate change on forest insect and pathogen impacts. Forestry 89:245–252. doi: 10.1093/forestry/cpw018

Reich PB, Lee TD, Hobbie SE (2014) Plant growth enhancement by elevated CO2 eliminated by joint water and nitrogen limitation.

Reyes-Fox M, Steltzer H, Trlica MJ, et al (2014) Elevated CO2 further lengthens growing season under warming conditions. Nature 510:259–62. doi: 10.1038/nature13207

Schlesinger W, Bernhardt E, Delucia EH, et al (2006) The Duke Forest FACE experiment: CO2 enrichment of a loblolly pine forest. Ecol Stud 187:197–212. doi: DOI: 10.1007/3-540-31237-4_11

Schlesinger WH, Bernhardt EH (2013) Biogeochemistry: An Analysis of Global Change.

Academic Press Inc.

Schmidt MWI, Torn MS, Abiven S, et al (2011) Persistence of soil organic matter as an ecosystem property. Nature 478:49–56. doi: 10.1038/nature10386

Shahzad T, Chenu C, Genet P, et al (2015) Contribution of exudates, arbuscular mycorrhizal fungi and litter depositions to the rhizosphere priming effect induced by grassland species. Soil Biol Biochem 80:146–155. doi: 10.1016/j.soilbio.2014.09.023

Smitley D, Davis T, Rebek E (2008) Progression of ash canopy thinning and dieback outward from the initial infestation of emerald ash borer (Coleoptera: Buprestidae) in southeastern Michigan. J Econ Entomol 101:1643–1650. doi: 10.1603/0022-0493(2008)101[1643:POACTA]2.0.CO;2

Springer CJ, Thomas RB (2007) Photosynthetic responses of forest understory tree species to long-term exposure to elevated carbon dioxide concentration at the Duke Forest FACE experiment. Tree Physiol 27:25–32. doi: 10.1093/treephys/27.1.25

Torn MS, Trumbore SE, Chadwick OA, et al (1997) Mineral control of soil organic carbon storage and turnover. Nature 389:3601–3603. doi: 10.1038/38260

van der Sleen P, Groenendijk P, Vlam M, et al (2015) No growth stimulation of tropical trees by 150 years of CO2 fertilization but water-use efficiency increased. Nat Geosci 8:24–28. doi: 10.1038/ngeo2313

Veres Z, Kotroczó Z, Fekete I, et al (2015) Soil extracellular enzyme activities are sensitive indicators of detrital inputs and carbon availability. Appl Soil Ecol 92:18–23. doi: 10.1016/j.apsoil.2015.03.006

Ward EJ, Oren R, Bell DM, et al (2013) The effects of elevated CO2 and nitrogen fertilization on stomatal conductance estimated from 11 years of scaled sap flux measurements at Duke

FACE. Tree Physiol 33:135–151. doi: 10.1093/treephys/tps118

White L, Luo Y (2002) Estimation of carbon transfer coefficients using Duke Forest free-air CO2 enrichment data. Appl Math Comput 130:101–120. doi: 10.1016/S0096-3003(01)00085-6

Wieder WR, Cleveland CC, Smith WK, Todd-Brown K (2015) Future productivity and carbon storage limited by terrestrial nutrient availability. Nat Geosci 8:441-U35. doi: 10.1038/ngeo2413

Zhu B, Gutknecht JLM, Herman DJ, et al (2014) Rhizosphere priming effects on soil carbon and nitrogen mineralization. Soil Biol Biochem 76:183–192. doi: 10.1016/j.soilbio.2014.04.033

TABLES AND FIGURES

Table 1 Chemical characteristics of both A-horizon (0 – 5 cm) bulk soil and density fractions from the DIRT plots at the UMBS site in 2014. Cells show mean values ± 1 SE (n = 3) and RB-ANOVA and post hoc test results, where capital letters represent cross-treatment differences ($\alpha <$ 0.05) for bulk soil analyses or for within density fractions (across columns within rows) and lower case letters represent cross-density fraction comparisons within treatments (across rows within columns). Marginally significant differences from Control are indicated by † ($0.05 < p <$ 0.10) and result from post hoc tests performed on data subsets by treatment and density fraction. "R" indicates a statistically significant ($\alpha = 0.05$) random block effect resulting from a RB-ANOVA, with a capital letter for treatment comparisons and a lowercase letter for fraction comparisons.

		Treatment		
Soil or Soil fraction	**-**	**No Input**	**Control**	**Double Litter**
Bulk soil	Mass (g • m^{-2})	4888 ± 1388 R†	5630 ± 457 R†	6119 ± 306 R†
	C (%)	7.1 ± 0.7 AR	9.5 ± 0.4 BR	9.6 ± 0.8 BR
	C (g • m^{-2})	328 ± 40 A	531 ± 57 B	570 ± 56 B
	N (%)	0.3 ± 0.1 AR†	0.6 ± 0.02 BR†	0.5 ± 0.1 BR†
	N (g • m^{-2})	15 ± 2 A	33 ± 4 B	30 ± 4 B
	C : N	21.1 ± 1.3	17.7 ± 0.6	20.1 ± 0.4
Free light fraction (<1.85 g • cm^{-3})	Mass (g • m^{-2})	825 ± 203 a	978 ± 211 a	984 ± 42 a
	C (%)	31.0 ± 1.5 a	33.2 ± 1.8 a	31.8 ± 3.5 ar†
	C (g • m^{-2})	253 ± 58 a	332 ± 87 a	311 ± 32 a
	δ^{13}C (‰)	-28.1 ± 0.2 R†	-26.9 ± 0.8 R†	-26.9 ± 1.2 R†
	N (%)	1.4 ± 0.1 Rar†	1.3 ± 0.1 Ra	1.2 ± 0.1 Ra
	N (g • m^{-2})	11 ± 2 a	13 ± 4	12 ± 1 a
	δ^{15}N (‰)	-2.8 ± 0.4	-2.7 ± 0.3	-2.8 ± 0.4
	C : N	26.6 ± 1.9	30.3 ± 0.8	29.8 ± 1.9 ra
Free light leachate	C (g • L)	0.03 ± 0.003 A	0.05 ± 0.009 B	0.06 ± 0.01 B
	N (g • L)	0.01 ± 0.002 A	0.017 ± 0.001 B	0.018 ± 0.001 B
Intermediate fraction (1.85 – 2.40 g • cm^{-3})	Mass (g • m^{-2})	577 ± 223 Ra	586 ± 205 Ra	534 ± 137 Ra
	C (%)	14.5 ± 5.2 Rb	11.8 ± 6.0 Rb	16.9 ± 5.7 Rbr†
	C (g • m^{-2})	67 ± 35 b	50 ± 14 b	77 ± 22 b
	δ^{13}C (‰)	-25.5 ± 1.8	-27.0 ± 0.3	-27.3 ± 0.1
	N (%)	0.7 ± 0.3 Rbr†	0.5 ± 0.2 Rb	0.6 ± 0.2 Rb
	N (g • m^{-2})	4 ± 2 b	2 ± 1	3 ± 1 b
	δ^{15}N (‰)	-1.2 ± 0.7	-1.2 ± 0.3	-2.7 ± 0.5
	C : N	23.0 ± 0.8 A	26.0 ± 1.7 A	29.9 ± 1.0 B ra
Dense fraction (>2.40 g • cm^{-3})	Mass (g • m^{-2})	3712 ± 1126 Rb	4010 ± 356 Rb	4925 ± 419 Rb
	C (%)	0.3 ± 0.2 c	0.1 ± 0.01 b	0.1 ± 0.01 cr†
	C (g • m^{-2})	11 ± 8 R†b†	4 ± 1 R†b	5 ± 1 R†b
	δ^{13}C (‰)	-27.0 ± 0.2	-26.4 ± 0.1	-26.8 ± 0.1
	N (%)	0.0 ± 0.002 cr†	0.0 ± 0.001 b	0.0 ± 0.001 c
	N (g • m^{-2})	0 ± 0.1 b	0 ± 0.1	0 ± 0.04 b
	δ^{15}N (‰)	-0.7 ± 0.8	-2.1 ± 0.6	-2.6 ± 0.3
	C : N	26.3 ± 11.6	30.3 ± 2.3	36.5 ± 2.6 rb

Table 2 Recovery of bulk mass, carbon (C), and nitrogen (N) in final soil fractions after sequential density fractionation of A-horizons of DIRT plots at the UMBS site in 2015. Cells show mean values ± 1 SE (n = 3), RB-ANOVA and Tukey's HSD test results, where capital letters represent cross-treatment differences ($\alpha < 0.05$). Marginally significant differences from Control are indicated by † ($0.05 < p < 0.10$) resulting from a post-hoc Tukey's HSD multiple comparisons test performed on data subsets by treatment. "R" indicates a statistically significant ($\alpha = 0.05$) random block effect resulting from a RB-ANOVA, with a capital letter for treatment comparisons and a lowercase letter for fraction comparisons.

		Recovery as proportion of bulk soil (%)		
		Treatment		
-	Density fraction (g • cm^{-3})	No Input	Control	Double Litter
Mass	Free light (< 1.85)	18 ± 2 Ra	17 ± 3 Ra	16 ± 1 Ra
	Intermediate (1.85 – 2.40)	11 ± 2 R†a	9 ± 2 R†a	9 ± 3 R†a
	Dense (> 2.40)	74 ± 3 ARb	71 ± 4 ARb	80 ± 3 BRb
	Total (sum)	*103 ± 4*	*98 ± 3*	*106 ± 4*
C	Free light (< 1.85)	78 ± 2 Aa	61 ± 12 ABa	54 ± 2 B†ar†
	Intermediate (1.85 – 2.40)	19 ± 7 b	10 ± 3 b	13 ± 3 br†
	Dense fraction (> 2.40)	3 ± 2 b	1 ± 0.1 b	1 ± 0.2 cr†
	Total (sum)	*100 ± 3*	*72 ± 11*	*69 ± 5*
N	Free light (< 1.85)	72 ± 1 Aa	39 ± 9 Ba	40 ± 2 Ba
	Intermediate (1.85 – 2.40)	21 ± 9 b	7 ± 2 b	10 ± 2 b
	Dense (> 2.40)	0.5 ± 0.1 Rb	1 ± 0.1 Rb	2 ± 1 Rc
	Total (sum)	*95 ± 9*	*46 ± 8*	*51 ± 4*

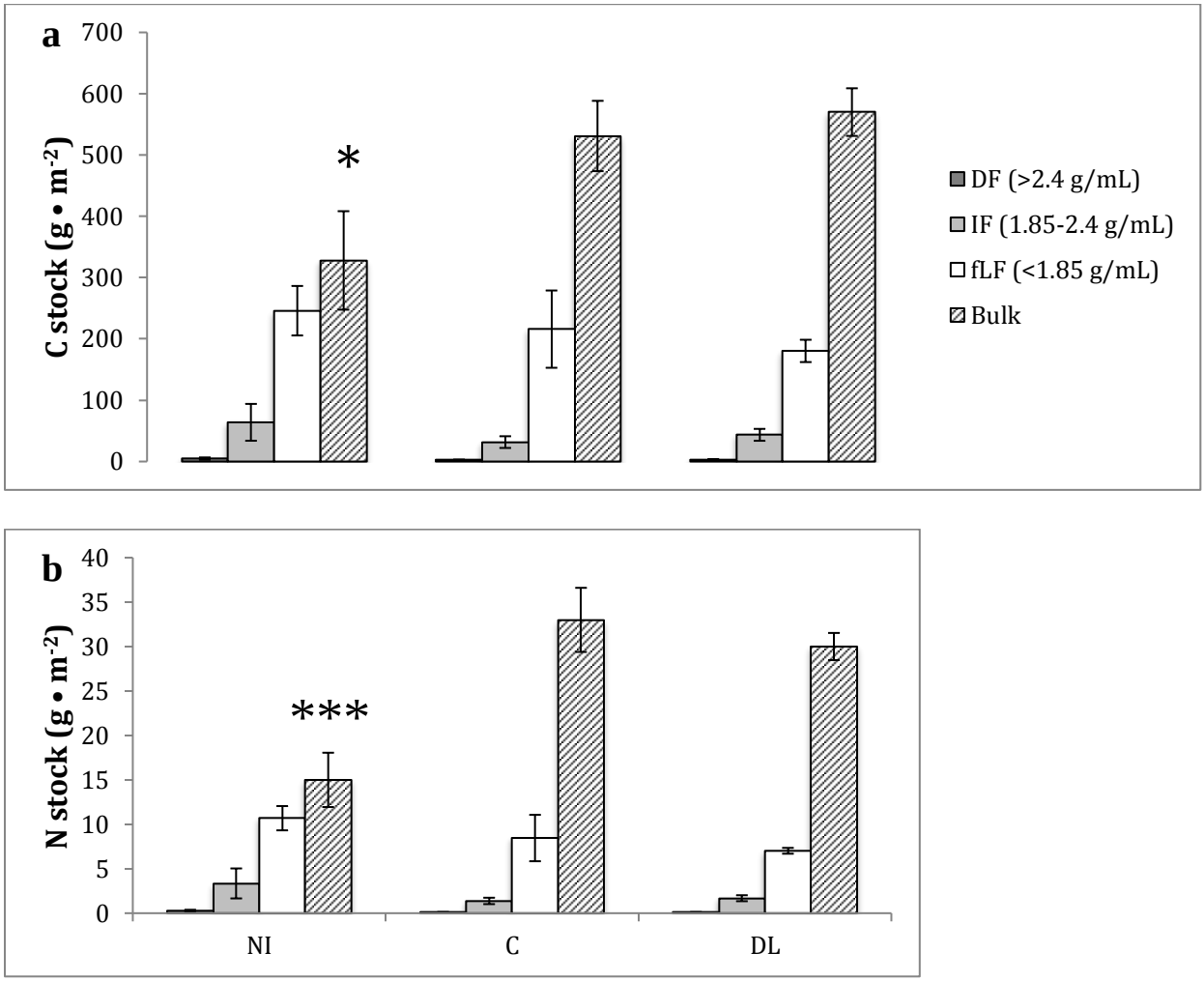

Fig 1 Total A-horizon stocks of **a** carbon (C) and **b** nitrogen (N) calculated using density fraction mass densities and their concentrations of C and N from UMBS DIRT plots in 2014, after 10 years of detrital manipulation. Bars showing bulk C and N (striped) were calculated separately using bulk C and N concentrations and mass densities, and resulted in larger total stock values than the sum of those recovered from density fractions. Bars show means ± 1 SE (n = 3; 1 composite soil sample per plot across 3 random blocks) for the free light (fLF), intermediate (IF), and densest (DF) density fraction within the No Input (NI), Control (C), and Double Litter (DL) treatments. Asterisks (*) are used to indicated significant differences compared to the Control mean of the same category (* = $p < 0.05$, *** = $p < 0.001$).

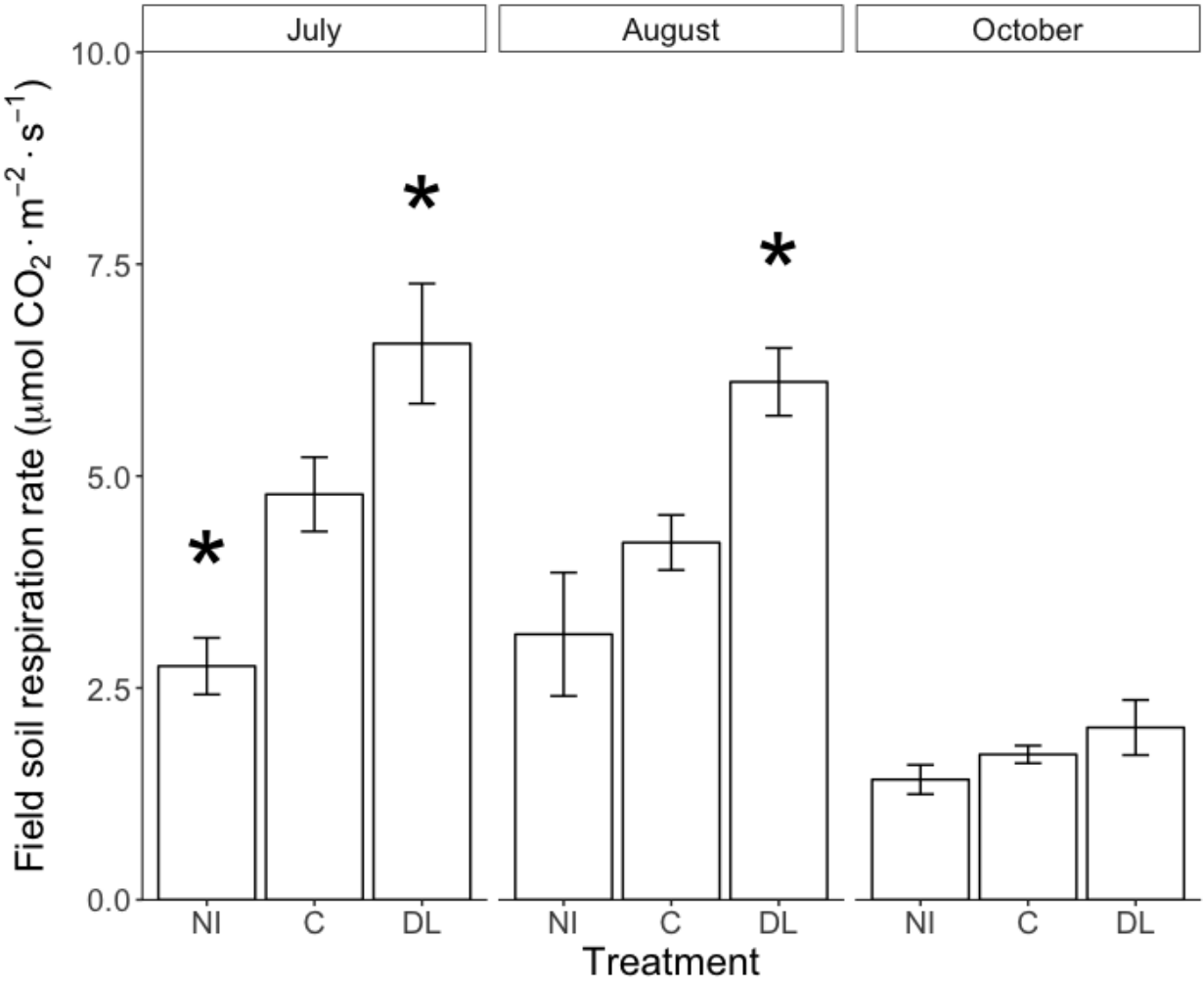

Fig 2 Field soil respiration from UMBS DIRT plots during 2014. Panels show the mean CO_2 efflux rates ± 1 SEM (n = 3; 1 respiration collar per plot across 3 random blocks) for Control (C), Double Litter (DL), and No Input (NI) treatments (respectively) for 1 sampling date per month in July, August, and October (respectively). Single asterisks indicate statistically significant differences (α = 0.05) from Control resulting from a Dunnett-type multiple comparisons post-hoc test performed on a linear mixed effects model for each date.

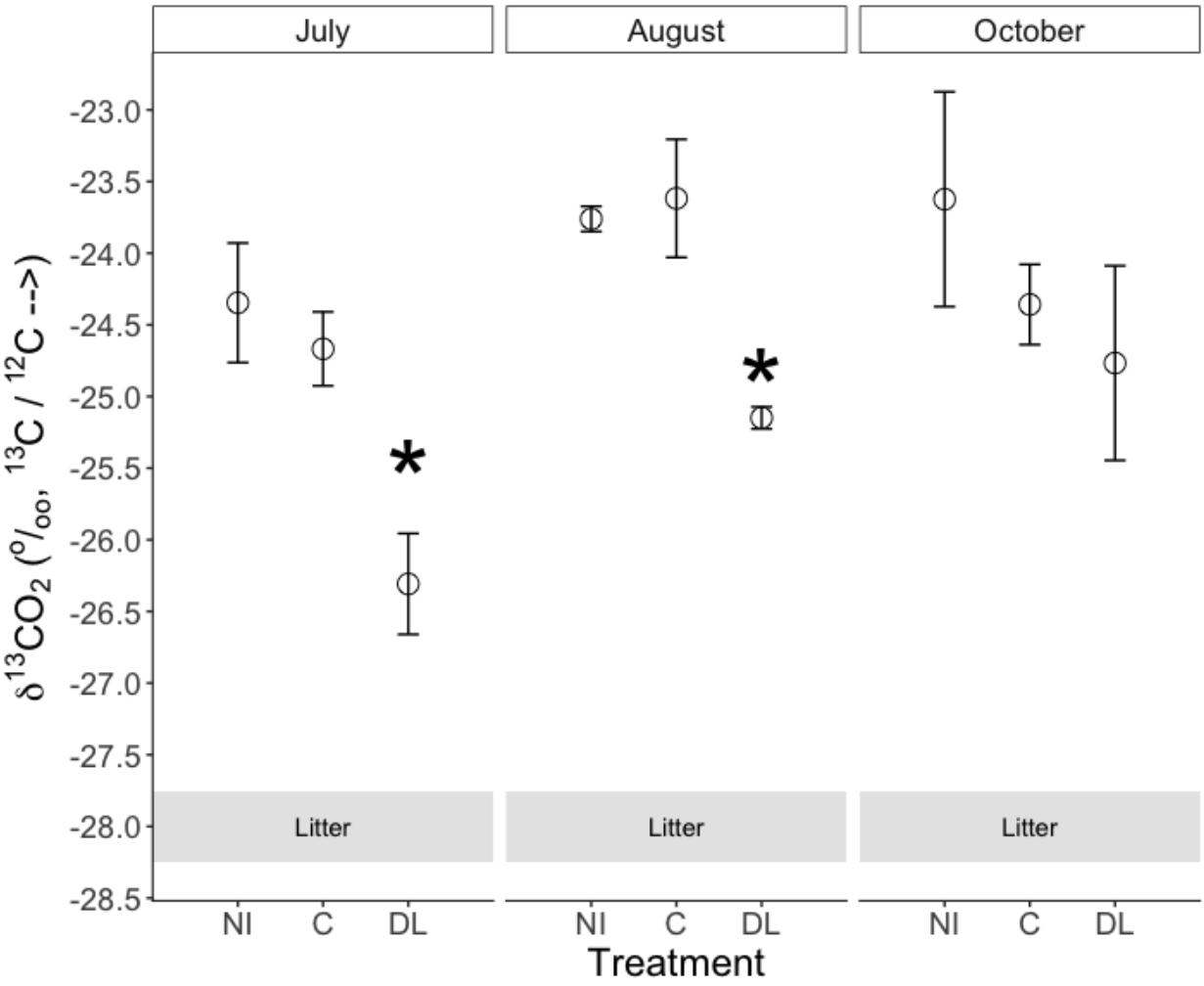

Fig 3 $\delta^{13}CO_2$ values for field soil respiration of UMBS DIRT plots during 2014. Panels show the mean value ± 1 SEM (n = 3; 1 respiration collar per plot across 3 random blocks) for Control (C), Double Litter (DL), and No Input (NI) treatments (respectively) for 1 sampling date per month in July, August, and October (respectively). Gray bars indicate average leaf $\delta^{13}C$ signature for the UMBS DIRT site. Asterisks (*) indicate statistically significant differences (α = 0.05) from Control resulting from a Dunnett-type multiple comparisons post-hoc test performed on a linear mixed effects model for each date.

SUPPLEMENTARY INFORMATION

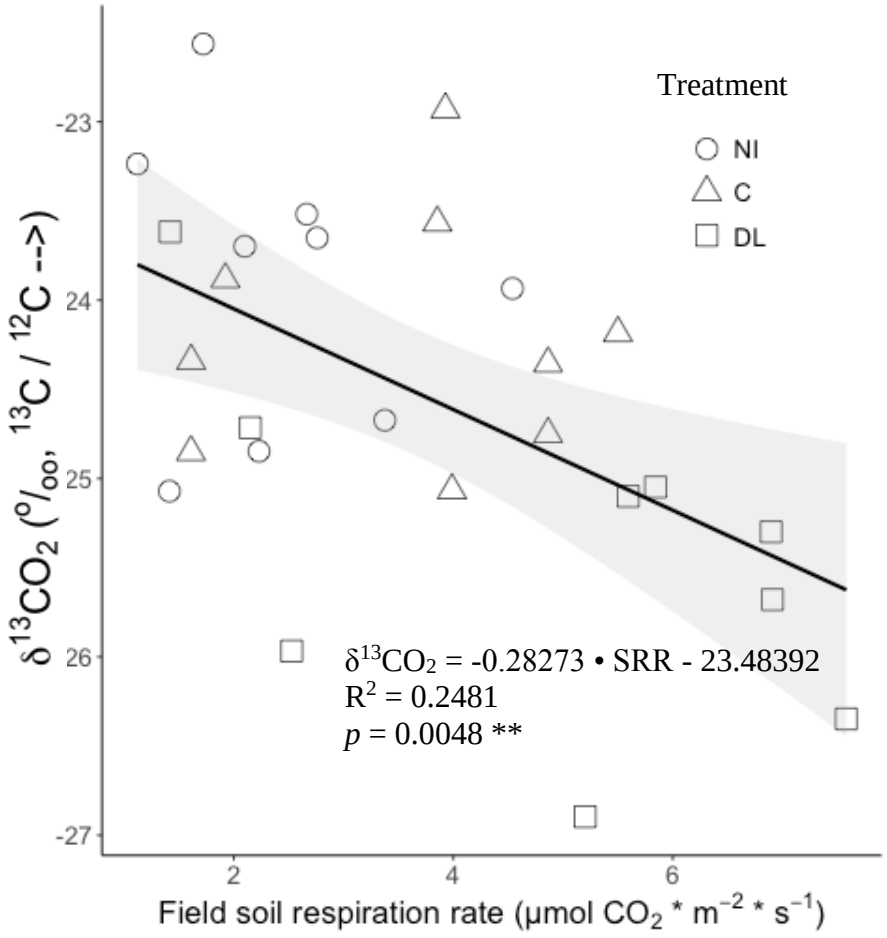

Fig S1 Correlation between field soil respiration rate and concentration-independent $\delta^{13}CO_2$ signatures of each respiration collar measured at the UMBS DIRT site throughout July, August, and October 2014, shown by treatment collar means (treated as independent data points for soil respiration rate in this regression: $n = 9$): No Input (NI), Control (C), and Double Litter (DL).

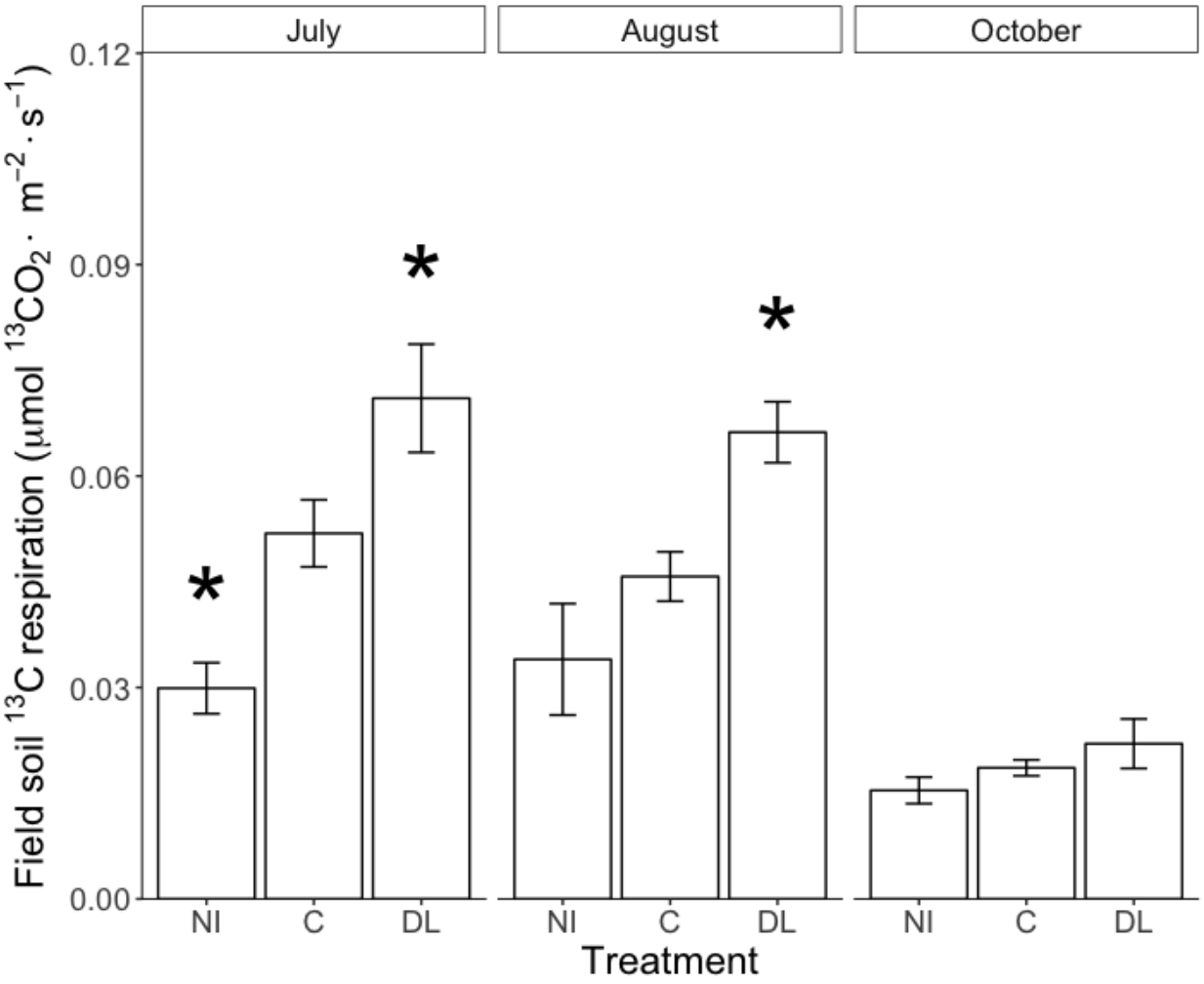

Fig S2 Field $^{13}CO_2$ mass efflux (calculated using isotopic ratio mass balance) from UMBS DIRT plots during 2014. Panels show mean rates ± 1 SEM (n = 3; 1 respiration collar per plot across 3 random blocks) for No Input (NI), Control (C), and Double Litter (DL) treatments (respectively) for 1 sampling date per month in July, August, and October (respectively). Single asterisks (*) indicate statistically significant differences (α = 0.05) from Control resulting from a Dunnett-type multiple comparisons post-hoc test performed on a linear mixed effects model for each date.

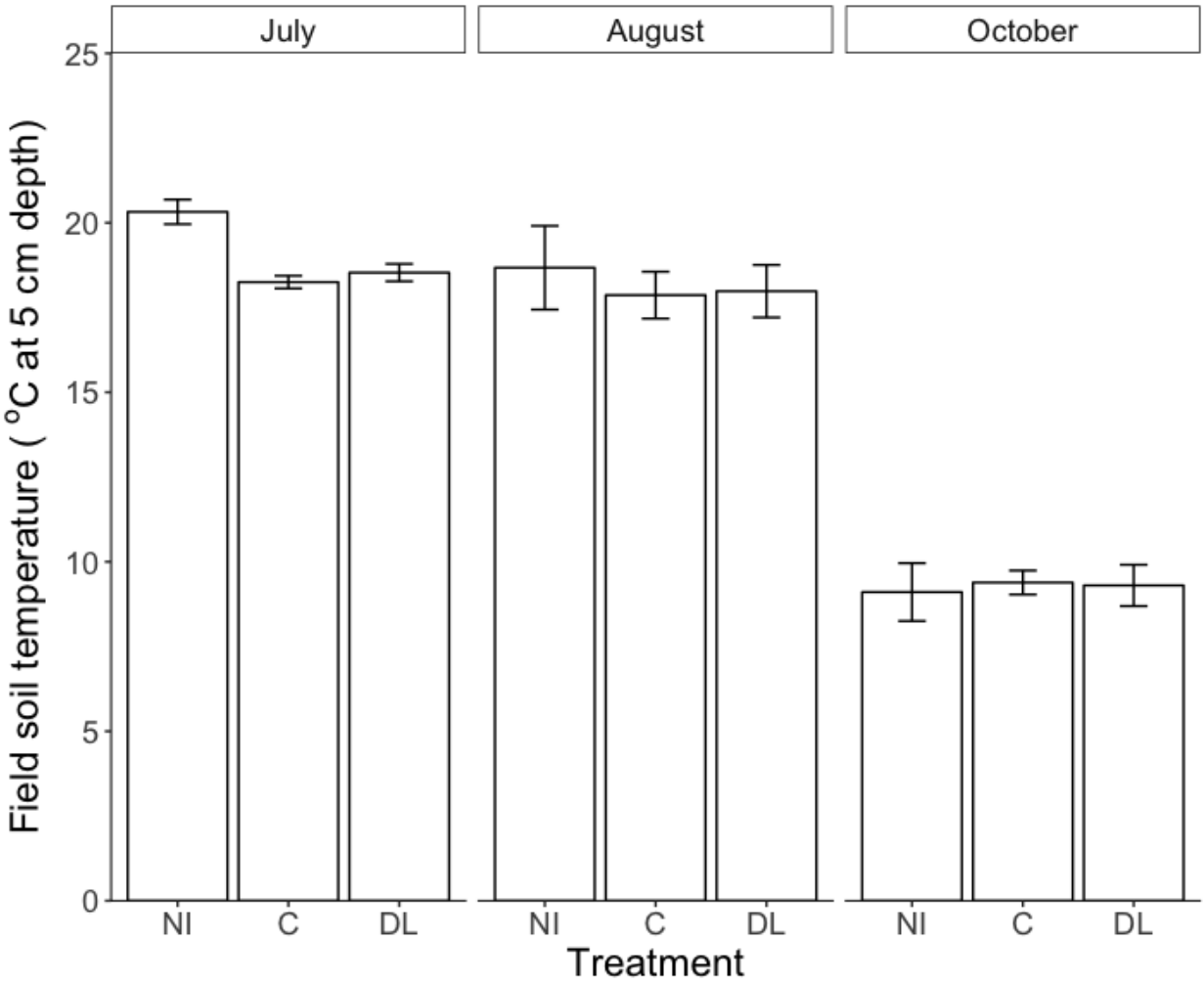

Fig S3 Field soil temperature at 5 cm depth from UMBS DIRT plots during 2014. Panels show mean values ± 1 SE (*n* = 3; 1 measurement per plot across 3 random blocks) for No Input (NI), Control (C), and Double Litter (DL) treatments during July, August, and October.

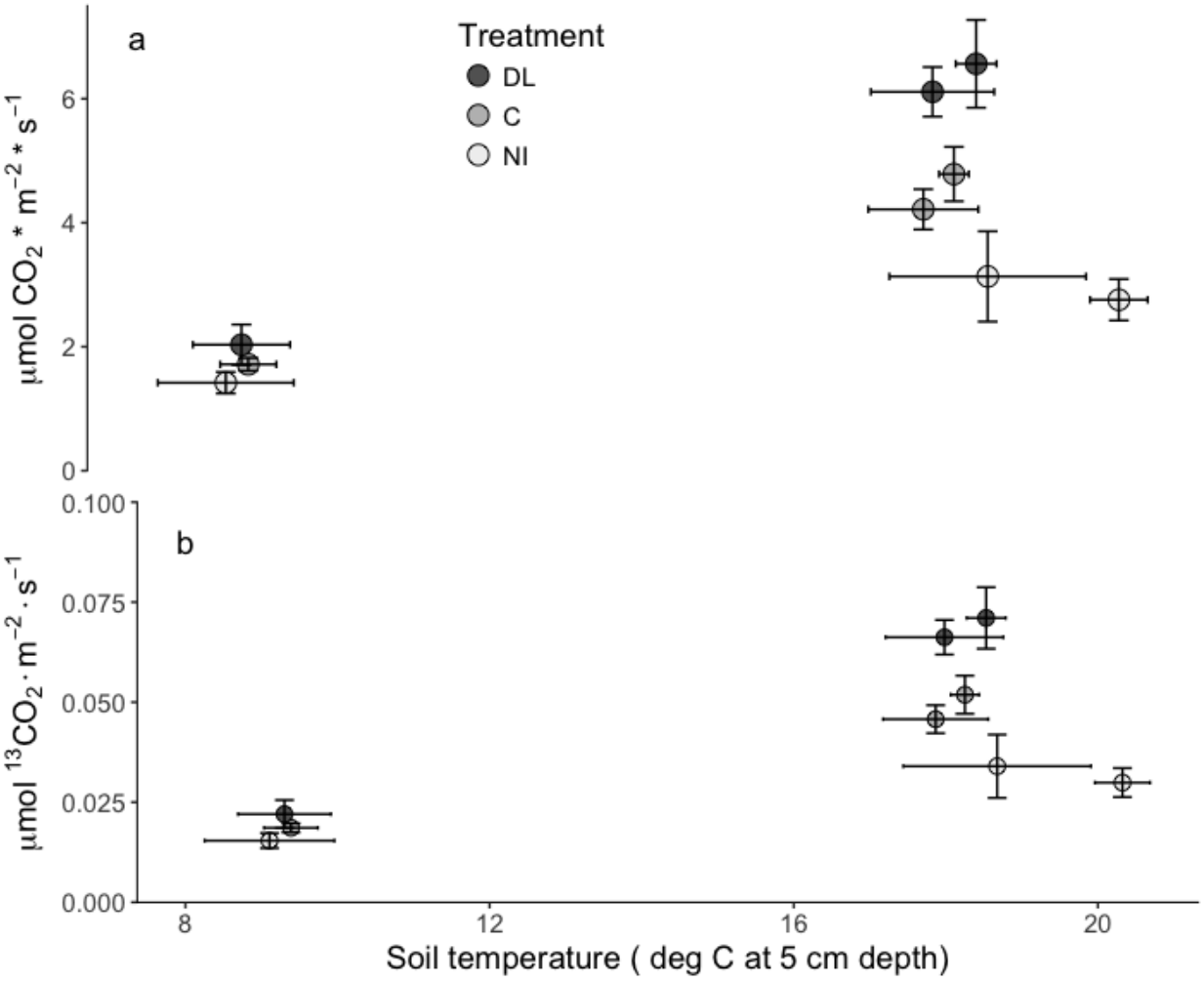

Fig S4 a Field soil respiration and **b** field soil $^{13}CO_2$ efflux rate plotted against field soil temperature at 5 cm depth for UMBS DIRT plots during 2014. Points show mean values ± 1 SE (n = 3; 1 respiration collar per plot across 3 random blocks) for No Input (NI), Control (C), and Double Litter (DL) treatments.

Table S1 Average field soil respiration from select DIRT plots at the UMBS site during 2014. Cells show mean values ± 1 SE ($n = 3$) and Tukey's HSD test results post-hoc to a RB-ANOVA with a (discrete) temperature-by-treatment interaction term. Significance categories ($\alpha = 0.05$, $p < 0.05$) are denoted by capital letters and apply to all cross-row comparisons. Low temperature group values recorded were in October and High temperatures include values were recorded in July and August.

Treatment	Soil temperature (at 5 cm depth)	Field soil respiration (μmol $CO_2 \bullet m^{-1} \bullet s^{-1}$)
No Input	Low (Fall)	1.42 ± 0.17 A
	High (Summer)	2.94 ± 0.37 A
Control	Low (Fall)	1.72 ± 0.10 A
	High (Summer)	4.50 ± 0.28 B
Double Litter	Low (Fall)	2.03 ± 0.33 A
	High (Summer)	6.34 ± 0.38 C

APPENDIX

Tables show results from statistical tests performed that yielded significant differences among values, including symbols indicating significance: *** = $p < 0.001$, ** = $p < 0.01$, * = $p < 0.05$, and . = $p < 0.10$. Most tests are Random Block Analyses of Variance (RB-ANOVA), and post hoc tests are generalized linear Dunnett comparisons of linear mixed effects models with "Block" as the assumed random effect, except in cases when fraction effects were being tested or when RB-ANOVA results indicated significant block effects in addition to treatment effects, when Tukey's Honest Significant Difference Test was used to minimize overestimation of treatments effects and perform all possible pairwise comparisons.

Table 1: A-horizon density fraction chemistry

RB-ANOVA: Mass density ~ treatment + random block

	D_f	*SS*	*MS*	*F*	*p*
Treatment	2	2306025	1153012	0.767	0.512
Block	1	5852913	5852913	3.894	0.105 .
Residuals	5	7515783	1503157		

Shapiro-Wilk normality test on above RB-ANOVA residuals:

W	*p*
0.96261	0.8252

RB-ANOVA: Bulk %C ~ treatment + random block

	D_f	*SS*	*MS*	*F*	*p*
Treatment	2	11.547	5.773	10.39	0.0166 *
Block	1	7.935	7.935	14.28	0.0129 *
Residuals	5	2.778	0.556		

Shapiro-Wilk normality test on above RB-ANOVA residuals:

W	*p*
0.92833	0.4656

Tukey's Honest Significant Difference Test of above RB-ANOVA factors:

Treatment	*Difference*	*Lower*	*Upper*	*p adjusted*
Double Litter – Control	0.1333333	-1.847132	2.1137987	0.9740275
No Input – Control	-2.3333333	-4.313799	-0.3528680	0.0274935 *
No Input – Double Litter	-2.4666667	-4.447132	-0.4862013	0.0221934 *

RB-ANOVA: Bulk C ~ treatment + random block

	D_f	*SS*	*MS*	*F*	*p*
Treatment	2	101294	50647	3.891	0.0957 .
Block	1	2440	2440	0.187	0.6831
Residuals	5	65090	13018		

Shapiro-Wilk normality test on above RB-ANOVA residuals:

W	*p*
0.93869	0.5682

Dunnett-type post-hoc general linear hypothesis test of linear mixed effects model:

	Estimate	*SEM*	*z*	*p*
(Intercept) == 0	531.00	61.25	8.669	<0.0001 ***
Double Litter == 0	39.00	80.01	0.487	0.9169
No Input == 0	-203.00	80.01	-2.537	0.0282 *

RB-ANOVA: Bulk %N ~ treatment + random block

	D_f	*SS*	*MS*	*F*	*p*
Treatment	2	0.10889	0.05444	23.333	0.00291 **
Block	1	0.01500	0.01500	6.429	0.05218 .
Residuals	5	0.01167	0.00233		

Shapiro-Wilk normality test on linear mixed effects model residuals:

W	*p*
0.90561	0.2863

Dunnett-type post-hoc general linear hypothesis test of linear mixed effects model:

	Estimate	*SEM*	*z*	*p*
(Intercept) == 0	0.60000	0.03849	15.588	<0.001 ***
Double Litter == 0	-0.10000	0.04303	-2.324	0.0523 .
No Input == 0	-0.26667	0.04303	-6.197	<0.001 ***

RB-ANOVA: Bulk N ~ treatment + random block

	D_f	*SS*	*MS*	*F*	*p*
Treatment	2	558.0	279.00	9.976	0.018 *
Block	1	8.2	8.17	0.292	0.612
Residuals	5	139.8	27.97		

Shapiro-Wilk normality test on linear mixed effects model residuals:

W	*p*
0.91228	0.3322

Dunnett-type post-hoc general linear hypothesis test of linear mixed effects model:

	Estimate	*SEM*	*z*	*p*
(Intercept) == 0	33.00	2.867	11.509	<0.0001 ***
Double Litter == 0	-3.00	3.037	-0.988	0.628
No Input == 0	-18.00	3.037	-5.927	<0.0001 ***

RB-ANOVA: free light fraction $\delta^{13}C$ ~ treatment + random block

	D_f	*SS*	*MS*	*F*	*p*
Treatment	2	2.802	1.401	1.125	0.3950
Block	1	5.607	5.607	4.502	0.0873 .
Residuals	5	6.227	1.245		

Shapiro-Wilk normality test on above RB-ANOVA residuals:

W	*P*
0.93851	0.5663

RB-ANOVA: free light fraction %N ~ treatment + random block

	D_f	*SS*	*MS*	*F*	*p*
Treatment	2	0.04667	0.02333	2.258	0.2001
Block	1	0.08167	0.08167	7.903	0.0375 *
Residuals	5	0.05167	0.01033		

Shapiro-Wilk normality test on above RB-ANOVA residuals:

W	*p*
0.94413	0.626

RB-ANOVA: Intermediate fraction mass density ~ treatment + random block

	D_f	*SS*	*MS*	*F*	*p*
Treatment	2	4594	2297	0.045	0.9567
Block	1	405080	405080	7.873	0.0377 *
Residuals	5	257247	51449		

Shapiro-Wilk normality test on above RB-ANOVA residuals:

W	*p*
0.94052	0.5874

RB-ANOVA: Intermediate fraction %C ~ treatment + random block

	D_f	*SS*	*MS*	*F*	*p*
Treatment	2	0.00892	0.00446	0.396	0.6926
Block	1	0.07472	0.07472	0.629	0.0498 *
Residuals	5	0.05636	0.01127		

Shapiro-Wilk normality test on above RB-ANOVA residuals:

W	*p*
0.94276	0.6112

RB-ANOVA: intermediate fraction %N ~ treatment + random block

	D_f	*SS*	*MS*	*F*	*p*
Treatment	2	0.0822	0.0411	0.67	0.5522
Block	1	0.8067	0.8067	13.15	0.0151 *
Residuals	5	0.3067	0.0613		

Shapiro-Wilk normality test on above RB-ANOVA residuals:

W	*p*
0.94228	0.6061

RB-ANOVA: Intermediate fraction C:N ~ treatment + random block

	D_f	*SS*	*MS*	*F*	*p*
Treatment	2	70.51	35.25	7.096	0.0346 *
Block	1	2.16	2.16	0.435	0.5388
Residuals	5	24.84	4.97		

Shapiro-Wilk normality test on above RB-ANOVA residuals:

W	*p*
0.90969	0.3137

Dunnett-type post-hoc general linear hypothesis test of linear mixed effects model:

	Estimate	*SEM*	*z*	*p*
(Intercept) == 0	25.967	1.225	21.202	<0.001 ***
Double Litter == 0	3.900	1.701	2.293	0.0533 *
No Input == 0	-2.933	1.701	-1.724	0.1851 ***

RB-ANOVA: Dense fraction mass density ~ treatment + random block

	D_f	*SS*	*MS*	*F*	*p*
Treatment	2	2400236	1200118	1.602	0.2900
Block	1	5678428	5678428	7.579	0.0402 *
Residuals	5	3746216	749243		

Shapiro-Wilk normality test on above RB-ANOVA residuals:

W	*p*
0.94365	0.6208

RB-ANOVA: Dense fraction C ~ treatment + random block

	D_f	*SS*	*MS*	*F*	*p*
Treatment	2	1.556	0.778	0.224	0.8067
Block	1	16.667	16.667	4.808	0.0798 .
Residuals	5	17.33	3.467		

Shapiro-Wilk normality test on above RB-ANOVA residuals:

W	*P*
0.92531	0.438

RB-ANOVA: No Input mass density ~ fraction + random block

	D_f	*SS*	*MS*	*F*	*p*
Fraction	2	18228018	9114009	9.618	0.0193 *
Block	1	3420150	3420150	3.609	0.1159
Residuals	5	4738005	947601		

Shapiro-Wilk normality test on above RB-ANOVA residuals:

W	*p*
0.90594	0.2885

Tukey's Honest Significant Difference Test of above RB-ANOVA factors:

Treatment	*Difference*	*Lower*	*Upper*	*p adjusted*
Intermediate – Dense	-3135.0000	-5721.264	-548.7362	0.0246553 *
Free light – Dense	-2887.6667	-5473.930	-301.4029	0.0336394 *
Free light – Intermediate	247.3333	-2338.930	2833.5971	0.9485592

RB-ANOVA: No Input %C ~ fraction + random block

	D_f	*SS*	*MS*	*F*	*p*
Fraction	2	1419.1	709.5	26.294	0.00222 **
Block	1	42.7	42.7	1.581	0.26414
Residuals	5	134.9	27.0		

Shapiro-Wilk normality test on above RB-ANOVA residuals:

W	*p*
0.92118	0.4021

Tukey's Honest Significant Difference Test of above RB-ANOVA factors:

Treatment	*Difference*	*Lower*	*Upper*	*p adjusted*
Intermediate – Dense	14.30000	0.4985737	28.10143	0.0441289 *
Free light – Dense	30.73333	16.9319071	44.53476	0.0018293 **
Free light – Intermediate	16.43333	2.6319071	30.23476	0.0264068 *

RB-ANOVA: No Input C ~ fraction + random block

	D_f	*SS*	*MS*	*F*	*p*
Fraction	2	138122	69061	64.624	0.000268 ***
Block	1	1601	1601	1.498	0.275528
Residuals	5	5343	1069		

Shapiro-Wilk normality test on above RB-ANOVA residuals:

W	*p*
0.91566	0.3575

Tukey's Honest Significant Difference Test of above RB-ANOVA factors:

Treatment	*Difference*	*Lower*	*Upper*	*p adjusted*
Intermediate – Dense	71	-15.85228	157.8523	0.0964595 .
Free light – Dense	291	204.14772	377.8523	0.0002659 ***
Free light – Intermediate	220	133.14772	306.8523	0.0010061 ***

RB-ANOVA: No Input %N ~ fraction + random block

	D_f	*SS*	*MS*	*F*	*p*
Fraction	2	2.9139	1.4569	27.153	0.00206 **
Block	1	0.2384	0.2384	4.443	0.08886 .
Residuals	5	0.2683	0.0537		

Shapiro-Wilk normality test on above RB-ANOVA residuals:

W	*p*
0.92286	0.4164

Tukey's Honest Significant Difference Test of above RB-ANOVA factors:

Treatment	*Difference*	*Lower*	*Upper*	*p adjusted*
Intermediate – Dense	0.7266667	0.11124698	1.342086	0.0272645 *
Free light – Dense	1.3933333	0.77791365	2.008753	0.0016950 **
Free light – Intermediate	0.6666667	0.05124698	1.282086	0.0375948 *

RB-ANOVA: No Input N ~ fraction + random block

	D_f	*SS*	*MS*	*F*	*p*
Fraction	2	255.98	127.99	26.037	0.00227 **
Block	1	7.48	7.48	1.522	0.27214
Residuals	5	24.58	4.92		

Shapiro-Wilk normality test on above RB-ANOVA residuals:

W	*p*
0.94504	0.6358

Tukey's Honest Significant Difference Test of above RB-ANOVA factors:

Treatment	*Difference*	*Lower*	*Upper*	*p adjusted*
Intermediate – Dense	3.7	-2.190488	9.590488	0.1968955
Free light – Dense	12.7	6.809512	18.590488	0.0021212 **
Free light – Intermediate	9.0	3.109512	14.890488	0.0096740 **

RB-ANOVA: Control mass density ~ fraction + random block

	D_f	*SS*	*MS*	*F*	*p*
Fraction	2	21472736	10736368	59.247	0.00033 ***
Block	1	232854	232854	1.285	0.30839
Residuals	5	906070	181214		

Shapiro-Wilk normality test on above RB-ANOVA residuals:

W	*p*
0.87185	0.1287

Tukey's Honest Significant Difference Test of above RB-ANOVA factors:

Treatment	*Difference*	*Lower*	*Upper*	*p adjusted*
Intermediate – Dense	-3476	-4606.9827	-2345.017	0.0004026 ***
Free light – Dense	-3032	-4162.9827	-1901.017	0.0007707 ***
Free light – Intermediate	444	-686.9827	1574.983	0.4647903

RB-ANOVA: Control %C ~ fraction + random block

	D_f	*SS*	*MS*	*F*	*p*
Fraction	2	1690.5	845.2	24.226	0.00268 **
Block	1	63.4	63.4	1.816	0.23558
Residuals	5	174.4	34.9		

Shapiro-Wilk normality test on above RB-ANOVA residuals:

W	*p*
0.97274	0.9171

Tukey's Honest Significant Difference Test of above RB-ANOVA factors:

Treatment	*Difference*	*Lower*	*Upper*	*p adjusted*
Intermediate – Dense	11.7	-3.992941	27.39294	0.1262051
Free light – Dense	33.1	17.407059	48.79294	0.0023445 **
Free light – Intermediate	21.4	5.707059	37.09294	0.0154763 *

RB-ANOVA: Control C ~ fraction + random block

	D_f	*SS*	*MS*	*F*	*p*
Fraction	2	224715	112357	16.655	0.00615 **
Block	1	6801	6801	1.008	0.36145
Residuals	5	33731	6746		

Shapiro-Wilk normality test on above RB-ANOVA residuals:

W	*p*
0.95756	0.7725

Tukey's Honest Significant Difference Test of above RB-ANOVA factors:

Treatment	*Difference*	*Lower*	*Upper*	*p adjusted*
Intermediate – Dense	53.33333	-164.88314	271.5498	0.7218569
Free light – Dense	358.66667	140.45019	576.8831	0.0070886 **
Free light – Intermediate	305.33333	87.11686	523.5498	0.0139377 *

RB-ANOVA: Control %N ~ fraction + random block

	D_f	*SS*	*MS*	*F*	*p*
Fraction	2	2.4269	1.2135	20.781	0.00378 **
Block	1	0.1347	0.1347	2.307	0.18928
Residuals	5	0.2920	0.0584		

Shapiro-Wilk normality test on above RB-ANOVA residuals:

W	*p*
0.9791	0.9595

Tukey's Honest Significant Difference Test of above RB-ANOVA factors:

Treatment	*Difference*	*Lower*	*Upper*	*p adjusted*
Intermediate – Dense	0.4956667	-0.1463482	1.137681	0.1142536
Free light – Dense	1.2623333	0.6203185	1.904348	0.0032209 **
Free light – Intermediate	0.7666667	0.1246518	1.408681	0.0261153 *

RB-ANOVA: Control N ~ fraction + random block

	D_f	*SS*	*MS*	*F*	*p*
Fraction	2	341.9	170.97	15.224	0.00747 **
Block	1	13.2	13.20	1.176	0.32776
Residuals	5	56.2	11.23		

Shapiro-Wilk normality test on above RB-ANOVA residuals:

W	*p*
0.96761	0.8736

Tukey's Honest Significant Difference Test of above RB-ANOVA factors:

Treatment	*Difference*	*Lower*	*Upper*	*p adjusted*
Intermediate – Dense	2.466667	-6.436744	11.37008	0.6627396
Free light – Dense	14.133333	5.229923	23.03674	0.0082279 **
Free light – Intermediate	11.666667	2.763256	20.57008	0.0181658 *

RB-ANOVA: Double Litter mass density ~ fraction + random block

	D_f	*SS*	*MS*	*F*	*p*
Fraction	2	34528644	17264322	114.355	$6.69 \cdot 10^{-5}$ ***
Block	1	558760	558760	3.701	0.112
Residuals	5	754856	150971		

Shapiro-Wilk normality test on above RB-ANOVA residuals:

W	*p*
0.92404	0.4267

Tukey's Honest Significant Difference Test of above RB-ANOVA factors:

Treatment	*Difference*	*Lower*	*Upper*	*p adjusted*
Intermediate – Dense	-4340.0000	-5372.3027	-3307.697	0.0000876 ***
Free light – Dense	-3941.3333	-4973.6361	-2909.031	0.0001409 ***
Free light – Intermediate	398.6667	-633.6361	1430.969	0.4748143

RB-ANOVA: Double Litter %C ~ fraction + random block

	D_f	*SS*	*MS*	*F*	*p*
Fraction	2	1502.8	751.4	25.079	0.00247 **
Block	1	117.9	117.9	3.936	0.10405 .
Residuals	5	149.8	30.0		

Shapiro-Wilk normality test on above RB-ANOVA residuals:

W	*p*
0.98299	0.9779

Tukey's Honest Significant Difference Test of above RB-ANOVA factors:

Treatment	*Difference*	*Lower*	*Upper*	*p adjusted*
Intermediate – Dense	16.76667	2.224114	31.30922	0.0298413 *
Free light – Dense	31.63333	17.090781	46.17589	0.0020369 **
Free light – Intermediate	14.86667	0.324114	29.40922	0.0462817 *

RB-ANOVA: Double Litter C ~ fraction + random block

	D_f	*SS*	*MS*	*F*	*p*
Fraction	2	79043	39521	11.769	0.0128 *
Block	1	1067	1067	0.318	0.5974
Residuals	5	16791	3358		

Shapiro-Wilk normality test on above RB-ANOVA residuals:

W	*p*
0.87476	0.1382

Tukey's Honest Significant Difference Test of above RB-ANOVA factors:

Treatment	*Difference*	*Lower*	*Upper*	*p adjusted*
Intermediate – Dense	44.66667	-109.29374	198.6271	0.6391117
Free light – Dense	217.33333	63.37293	371.2937	0.0134433 *
Free light – Intermediate	172.66667	18.70626	326.6271	0.0330909 *

RB-ANOVA: Double Litter %N ~ fraction + random block

	D_f	*SS*	*MS*	*F*	*p*
Fraction	2	2.2698	1.1349	27.421	0.00202 **
Block	1	0.1064	0.1064	2.571	0.16975
Residuals	5	0.2069	0.0414		

Shapiro-Wilk normality test on above RB-ANOVA residuals:

W	*p*
0.97837	0.9554

Tukey's Honest Significant Difference Test of above RB-ANOVA factors:

Treatment	*Difference*	*Lower*	*Upper*	*p adjusted*
Intermediate – Dense	0.63	0.08950084	1.170499	0.0286370 *
Free light – Dense	1.23	0.68950084	1.770499	0.0016554 **
Free light – Intermediate	0.60	0.05950084	1.40499	0.0343686 *

RB-ANOVA: Double Litter N ~ fraction + random block

	D_f	*SS*	*MS*	*F*	*p*
Fraction	2	120.47	60.23	13.816	0.00919 **
Block	1	2.88	2.88	0.662	0.45299
Residuals	5	21.80	4.36		

Shapiro-Wilk normality test on above RB-ANOVA residuals:

W	*p*
0.90618	0.29

Tukey's Honest Significant Difference Test of above RB-ANOVA factors:

Treatment	*Difference*	*Lower*	*Upper*	*p adjusted*
Intermediate – Dense	1.853333	-3.694176	7.400842	0.5612510
Free light – Dense	8.520000	2.972491	14.067509	0.0094650 **
Free light – Intermediate	6.666667	1.119158	12.214176	0.0254891 *

RB-ANOVA: Double Litter C:N ~ fraction + random block

	D_f	*SS*	*MS*	*F*	*p*
Treatment	2	87.12	43.56	8.051	0.0273 *
Block	1	42.67	42.67	7.886	0.0376 *
Residuals	5	27.05	5.41		

Shapiro-Wilk normality test on above RB-ANOVA residuals:

W	*p*
0.96314	0.8305

Tukey's Honest Significant Difference Test of above RB-ANOVA factors:

Treatment	*Difference*	*Lower*	*Upper*	*p adjusted*
Intermediate – Dense	-6.600000	-12.779957	-0.4200428	0.0395883 *
Free light – Dense	-6.600000	-12.779957	-0.4200428	0.0395883 *
Free light – Intermediate	$-3.552714 \cdot 10^{-15}$	-6.179957	6.1799572	1.0000000

Table 2: Recovery of bulk soils after sequential density fractionation

% of bulk mass recovered as fLF ~ treatment + random block

	D_f	*SS*	*MS*	*F*	*p*
Treatment	2	3.56	1.78	0.285	0.7633
Block	1	48.17	48.17	7.727	0.0389 *
Residuals	5	31.17	6.23		

Shapiro-Wilk normality test on above RB-ANOVA residuals:

W	*p*
0.94174	0.6003

% of bulk mass recovered as IF ~ treatment + random block

	D_f	*SS*	*MS*	*F*	*p*
Treatment	2	2.00	1.00	0.093	0.9128
Block	1	60.17	60.17	5.588	0.0644 .
Residuals	5	53.83	10.77		

Shapiro-Wilk normality test on above RB-ANOVA residuals:

W	*p*
0.93314	0.5118

% of bulk mass recovered as DF ~ treatment + random block

	D_f	*SS*	*MS*	*F*	*p*
Treatment	2	124.2	62.11	8.066	0.0272 *
Block	1	121.5	121.5	15.779	0.0106 *
Residuals	5	38.5	7.70		

Shapiro-Wilk normality test on above RB-ANOVA residuals:

W	*p*
0.96059	0.8045

Tukey's Honest Significant Difference Test of above RB-ANOVA factors:

Treatment	*Difference*	*Lower*	*Upper*	*p adjusted*
DL – C	9.000000	1.627659	16.372341	0.0239909 *
NI – C	3.333333	-4.039008	10.705675	0.3782443
NI – DL	-5.666667	-13.039008	1.705675	0.1157229

% of bulk C recovered as fLF ~ treatment + random block

	D_f	*SS*	*MS*	*F*	*p*
Treatment	2	0.09076	0.04538	3.894	0.0956 .
Block	1	0.02940	0.02940	2.523	0.1731
Residuals	5	0.05827	0.01165		

Shapiro-Wilk normality test on above RB-ANOVA residuals:

W	*p*
0.96201	0.8192

Tukey's Honest Significant Difference Test of above RB-ANOVA factors:

Treatment	*Difference*	*Lower*	*Upper*	*p adjusted*
DL – C	-0.07333333	-0.36013730	0.2134706	0.7014595
NI – C	0.16666667	-0.12013730	0.4534706	0.2352259
NI – DL	0.24000000	-0.04680397	0.5268040	0.0898092 .

% of bulk N recovered as fLF ~ treatment + random block

	D_f	*SS*	*MS*	*F*	*p*
Treatment	2	0.21807	0.10903	17.001	0.00588 **
Block	1	0.01307	0.01307	2.037	0.21282
Residuals	5	0.03207	0.00641		

Shapiro-Wilk normality test on above RB-ANOVA residuals:

W	*p*
0.96771	0.8745

Tukey's Honest Significant Difference Test of above RB-ANOVA factors:

Treatment	*Difference*	*Lower*	*Upper*	*p adjusted*
DL – C	0.01333333	-0.1994325	0.2260992	0.9774413
NI – C	0.33666667	0.1239008	0.5494325	0.0083409 **
NI – DL	0.32333333	0.1105675	0.5360992	0.0098961 **

% N of bulk recovered as DF ~ treatment + random block

	D_f	*SS*	*MS*	*F*	*p*
Treatment	2	0.0001620	0.00008100	2.907	0.1454
Block	1	0.0001927	0.0001927	6.914	0.0466 *
Residuals	5	0.0001393	0.00002787		

Shapiro-Wilk normality test on above RB-ANOVA residuals:

W	*p*
0.96379	0.837

% of No Input bulk mass recovered ~ fraction + random block

	D_f	*SS*	*MS*	*F*	*p*
Fraction	2	0.7475	0.3737	254.826	$9.3 \cdot 10^{-6}$ ***
Block	1	0.0017	0.0017	1.136	0.335
Residuals	5	0.0073	0.0015		

Shapiro-Wilk normality test on above RB-ANOVA residuals:

W	*p*
0.93243	0.5049

Tukey's Honest Significant Difference Test of above RB-ANOVA factors:

Treatment	*Difference*	*Lower*	*Upper*	*p adjusted*
Intermediate – Dense	-0.6433333	-0.74508131	-0.5415854	0.0000135 ***
Free light – Dense	-0.5733333	-0.67508131	-0.4715854	0.0000214 ***
Free light – Intermediate	0.0700000	-0.03174798	0.1717480	0.1568947

% of No Input bulk C recovered ~ fraction + random block

	D_f	*SS*	*MS*	*F*	*p*
Fraction	2	0.9334	0.4667	72.918	0.0002 ***
Block	1	0.0003	0.0003	0.042	0.8463
Residuals	5	0.0320	0.0064		

Shapiro-Wilk normality test on above RB-ANOVA residuals:

W	*p*
0.94899	0.679

Tukey's Honest Significant Difference Test of above RB-ANOVA factors:

Treatment	*Difference*	*Lower*	*Upper*	*p adjusted*
Intermediate – Dense	0.1633333	-0.04921126	0.3758779	0.1157977
Free light – Dense	0.7500000	0.53745541	0.9625446	0.0002069 ***
Free light – Intermediate	0.5866667	0.37412207	0.7992113	0.0006715 ***

% of No Input bulk N recovered ~ fraction + random block

	D_f	*SS*	*MS*	*F*	*p*
Fraction	2	0.8003	0.4001	44.542	0.000651 ***
Block	1	0.0008	0.0008	0.091	0.775162
Residuals	5	0.0449	0.0090		

Shapiro-Wilk normality test on above RB-ANOVA residuals:

W	*p*
0.85392	0.08229 .

Tukey's Honest Significant Difference Test of above RB-ANOVA factors:

Treatment	*Difference*	*Lower*	*Upper*	*p adjusted*
Intermediate – Dense	0.1933333	-0.05848006	0.4451467	0.1161028
Free light – Dense	0.7066667	0.45485327	0.9584801	0.0006209 ***
Free light – Intermediate	0.5133333	0.26151994	0.7651467	0.0027367 **

% of Control bulk mass recovered ~ fraction + random block

	D_f	*SS*	*MS*	*F*	*p*
Fraction	2	0.6824	0.3412	114.882	$6.62 \bullet 10^{-5}$ ***
Block	1	0.0014	0.0014	0.455	0.53
Residuals	5	0.0149	0.0030		

Shapiro-Wilk normality test on above RB-ANOVA residuals:

W	*p*
0.91399	0.3448

Tukey's Honest Significant Difference Test of above RB-ANOVA factors:

Treatment	*Difference*	*Lower*	*Upper*	*p adjusted*
Intermediate – Dense	-0.62	-0.76478991	-0.4752101	0.0000799 ***
Free light – Dense	-0.54	-0.68478991	-0.3952101	0.0001580 ***
Free light – Intermediate	0.08	-0.06478991	0.2247899	0.2619029

% of Control bulk C recovered ~ fraction + random block

	D_f	*SS*	*MS*	*F*	*p*
Fraction	2	0.6356	0.3178	23.142	0.00297 **
Block	1	0.0216	0.0216	1.573	0.26524
Residuals	5	0.0687	0.0137		

Shapiro-Wilk normality test on above RB-ANOVA residuals:

W	*p*
0.97952	0.9618

Tukey's Honest Significant Difference Test of above RB-ANOVA factors:

Treatment	*Difference*	*Lower*	*Upper*	*p adjusted*
Intermediate – Dense	0.0900000	-0.2213494	0.4013494	0.6410115
Free light – Dense	0.6033333	0.2919839	0.9146828	0.0034381 **
Free light – Intermediate	0.5133333	0.2019839	0.8246828	0.0069945 **

% of Control bulk N recovered ~ fraction + random block

	D_f	*SS*	*MS*	*F*	*p*
Fraction	2	0.24780	0.12390	18.312	0.005 **
Block	1	0.01067	0.01067	1.577	0.265
Residuals	5	0.03383	0.00677		

Shapiro-Wilk normality test on above RB-ANOVA residuals:

W	*p*
0.97052	0.8991

Tukey's Honest Significant Difference Test of above RB-ANOVA factors:

Treatment	*Difference*	*Lower*	*Upper*	*p adjusted*
Intermediate – Dense	0.06233333	-0.15620799	0.2808747	0.6479434
Free light – Dense	0.37900000	0.16045868	0.5975413	0.0056176 **
Free light – Intermediate	0.31666667	0.09812535	0.5352080	0.0120708 *

% of Double Litter bulk mass recovered ~ fraction + random block

	D_f	*SS*	*MS*	*F*	*p*
Fraction	2	0.9224	0.4612	272.369	$7.89 \bullet 10^{-6}$ ***
Block	1	0.0017	0.0017	0.984	0.367
Residuals	5	0.0085	0.0017		

Shapiro-Wilk normality test on above RB-ANOVA residuals:

W	*p*
0.90139	0.2602

Tukey's Honest Significant Difference Test of above RB-ANOVA factors:

Treatment	*Difference*	*Lower*	*Upper*	*p adjusted*
Intermediate – Dense	-0.71000000	-0.81932798	-0.6006720	0.0000123 ***
Free light – Dense	-0.64333333	-0.75266131	-0.5340054	0.0000178 ***
Free light – Intermediate	0.06666667	-0.04266131	0.1759946	0.2110732

% of Double Litter bulk C recovered ~ fraction + random block

	D_f	*SS*	*MS*	*F*	*p*
Fraction	2	0.4615	0.23074	310.419	$5.71 \cdot 10^{-6}$ ***
Block	1	0.0038	0.00375	5.045	0.0746 .
Residuals	5	0.0037	0.00074		

Shapiro-Wilk normality test on above RB-ANOVA residuals:

W	*p*
0.97073	0.9009

Tukey's Honest Significant Difference Test of above RB-ANOVA factors:

Treatment	*Difference*	*Lower*	*Upper*	*p adjusted*
Intermediate – Dense	0.1233333	0.05089776	0.1957689	0.0060854 **
Free light – Dense	0.5300000	0.45756443	0.6024356	0.0000081 ***
Free light – Intermediate	0.4066667	0.33423110	0.4791022	0.0000217 ***

% of Double Litter bulk N recovered ~ fraction + random block

	D_f	*SS*	*MS*	*F*	*p*
Fraction	2	0.25386	0.12693	131.365	$4.77 \bullet 10^{-5}$ ***
Block	1	0.00047	0.00047	0.485	0.517
Residuals	5	0.00483	0.00097		

Shapiro-Wilk normality test on above RB-ANOVA residuals:

W	*p*
0.97262	0.9162

Tukey's Honest Significant Difference Test of above RB-ANOVA factors:

Treatment	*Difference*	*Lower*	*Upper*	*p adjusted*
Intermediate – Dense	0.0890000	0.006415017	0.1715850	0.0383101 *
Free light – Dense	0.3923333	0.309748350	0.4749183	0.0000477 ***
Free light – Intermediate	0.3033333	0.220748350	0.3859183	0.0001702 ***

Fig 1: Bulk and density fraction C and N across treatments

Shapiro-Wilk normality test on linear mixed effects model residuals:

W	*p*
0.93869	0.5682

Bulk C ~ treatment + random block

	D_f	*SS*	*MS*	*F*	*p*
Treatment	2	101294	50647	3.891	0.0957 .
Block	1	2440	2440	0.187	0.6831
Residuals	4	65090	13018		

Dunnett-type post-hoc general linear hypothesis test:

	Estimate	*SEM*	*z*	*p*
(Intercept) == 0	531.00	61.25	8.669	<0.0001 ***
Double Litter == 0	39.00	80.01	0.487	0.9169
No Input == 0	-203.00	80.01	-2.537	0.028 *

Shapiro-Wilk normality test on linear mixed effects model residuals:

W	*p*
0.91228	0.3322

Bulk N ~ treatment + random block

	D_f	*SS*	*MS*	*F*	*p*
Treatment	2	558.0	279.00	9.976	0.018 .
Block	1	8.2	8.17	0.292	0.612
Residuals	4	139.8	27.97		

Dunnett-type post-hoc general linear hypothesis test:

	Estimate	*SEM*	*z*	*p*
(Intercept) == 0	33.00	2.867	11.509	<0.0001 ***
Double Litter == 0	-3.00	3.037	-0.988	0.628
No Input == 0	-18.00	3.037	-5.927	<0.0001 ***

Fig 2: Field soil respiration

July field CO_2 efflux ~ treatment + random block

	D_f	*SS*	*MS*	*F*	*p*
Treatment	2	21.762	10.881	9.137	0.0322 *
Block	2	0.068	0.034	0.029	0.9721
Residuals	4	4.763	1.191		

Shapiro-Wilk normality test on above RB-ANOVA residuals:

W	*p*
0.9848	0.9845

Dunnett-type post-hoc general linear hypothesis test of a linear mixed effects model:

glht (lmer (July CO_2 efflux ~ treatment + (1 | block → random effect))

	Estimate	*SEM*	*z*	*p*
Intercept == 0	4.7841	0.5181	9.234	< 0.001 ***
Double Litter == 0	1.7791	0.7327	2.428	0.0372 *
No Input == 0	-2.0272	0.7327	-2.767	0.0145 *

August field CO_2 efflux ~ treatment + random block

	D_f	*SS*	*MS*	*F*	*p*
Treatment	2	13.636	6.818	8.730	0.0347 *
Block	2	1.649	0.825	1.056	0.4283
Residuals	4	3.124	0.781		

Shapiro-Wilk normality test on above RB-ANOVA residuals:

W	*p*
0.9158	0.3587

Dunnett-type post-hoc general linear hypothesis test of a linear mixed effects model:

glht (lmer (August CO_2 efflux ~ treatment + (1 | block → random effect))

	Estimate	*SEM*	*z*	*p*
Intercept == 0	4.2156	0.5150	8.186	< 0.001 ***
Double Litter == 0	1.8955	0.7216	2.678	0.0219 *
No Input == 0	-1.0828	0.7216	-1.501	0.2776

Fig 3: Field soil respiration $\delta^{13}CO_2$

July field $\delta^{13}CO_2$ ~ treatment + random block

	D_f	*SS*	*MS*	*F*	*p*
Treatment	2	1.7351	0.8676	9.137	0.0322 *
Block	2	0.0054	0.0027	0.029	0.9721
Residuals	4	0.3798	0.0950		

Shapiro-Wilk normality test on above RB-ANOVA residuals:

W	*p*
0.9848	0.9845

Dunnett-type post-hoc general linear hypothesis test of a linear mixed effects model:

glht (lmer (July field $\delta^{13}CO_2$ ~ treatment + (1 | block → random effect))

	Estimate	*SEM*	*z*	*p*
Intercept == 0	-24.8348	0.1463	-169.763	< 0.001 ***
Double Litter == 0	-0.5024	0.2069	-2.428	0.0370 *
No Input == 0	0.5724	0.2069	2.767	0.0147 *

August field $\delta^{13}CO_2$ ~ treatment + random block

	D_f	*SS*	*MS*	*F*	*p*
Treatment	2	1.0872	0.5436	8.730	0.0347 *
Block	2	0.1315	0.0658	1.056	0.4283
Residuals	4	0.2491	0.0623		

Shapiro-Wilk normality test on above RB-ANOVA residuals:

W	*p*
0.9544	0.7386

Dunnett-type post-hoc general linear hypothesis test of a linear mixed effects model:

glht (lmer (August field $\delta^{13}CO_2$ ~ treatment + (1 | block → random effect))

	Estimate	*SEM*	*z*	*p*
Intercept == 0	-24.6743	0.1454	-169.689	< 0.001 ***
Double Litter == 0	-0.5352	0.2037	-2.627	0.0216 *
No Input == 0	0.3057	0.2037	1.501	0.2777

Table 1: Recovery bulk soil from sequential density fractionation

Arcsin (sqrt (yield)) ~ fraction + treatment + random block

	D_f	*SS*	*MS*	*F*	*p*
Fraction	2	2.7387	1.3694	453.970	$< 2x10^{-16}$ ***
Treatment	2	0.0001	0.0001	0.017	0.983
Block	1	0.0001	0.0001	0.028	0.868
Residuals	21	0.0633	0.0030		

Shapiro-Wilk normality test on above RB-ANOVA residuals:

W	*p*
0.9713	0.6368

Tukey's Honest Significant Difference Test of above RB-ANOVA factors:

Treatment	*Difference*	*Lower*	*Upper*	*p adjusted*
IF – fLF	-0.1121295	-0.1773880	-0.04687091	0.0008257 ***
DF – fLF	0.6125329	0.5472743	0.67779143	0.0000000 ***
DF - IF	0.7246623	0.6594038	0.78992091	0.0000000 ***

Ln (fLF [DOC]) ~ treatment + random block

	D_f	*SS*	*MS*	*F*	*p*
Treatment	2	0.7312	0.3656	8.877	0.0226 *
Block	1	0.1561	0.1561	3.790	0.1091
Residuals	5	0.2059	0.0412		

Shapiro-Wilk normality test on above RB-ANOVA residuals:

W	*p*
0.9128	0.3357

Dunnett-type post-hoc general linear hypothesis test of a linear mixed effects model:

glht (lmer (ln (fLF [DOC]) ~ treatment + (1 | block → random effect)))

	Estimate	*SEM*	*z*	*p*
Intercept == 0	8.3772	0.1418	59.070	< 0.0001 ***
No Input == 0	-0.4904	0.1188	-4.128	< 0.0001 ***
Double Litter == 0	0.1852	0.1188	1.559	0.284

Ln (fLF [TDN]) ~ treatment + random block

	D_f	*SS*	*MS*	*F*	*p*
Treatment	2	0.4215	0.21076	4.124	0.0875 .
Block	1	0.0334	0.03343	0.654	0.4554
Residuals	5	0.2555	0.05111		

Shapiro-Wilk normality test on above RB-ANOVA residuals:

W	*p*
0.9531	0.7238

Dunnett-type post-hoc general linear hypothesis test of a linear mixed effects model:

glht (lmer (ln (fLF [TDN]) ~ treatment + (1 | block → random effect)))

	Estimate	*SEM*	*z*	*p*
Intercept == 0	7.10615	0.12670	56.085	< 0.001 ***
No Input == 0	-0.44428	0.17918	-2.479	< 0.0322 *
Double Litter == 0	0.02831	0.17918	0.158	0.9961

Fig S1: $\delta^{13}CO_2$ versus CO_2 efflux (mass-dependent ^{13}C fractionation)

Field soil respiration $\delta^{13}CO_2$ ~ field soil CO_2 efflux

	Estimate	*SE*	*t*	*p*
(Intercept)	-23.48392	0.37376	-62.831	$< 2 \times 10^{-16}$ ***
CO_2 efflux	-0.28237	0.09123	-3.095	0.0048 **

Adj. $R^2 = 0.2481$

Table S2: Field soil temperature at 5 cm depth

Field CO_2 efflux ~ field temperature$_{(discrete)}$ * treatment + random block

	D_f	*SS*	*MS*	*F*	*p*
Temperature	1	49.49	49.49	83.914	2.12×10^{-8} ***
Treatment	2	27.42	13.71	23.250	7.83×10^{-6} ***
Block	2	0.28	0.14	0.239	0.7897
Temperature: Treatment	2	7.74	3.87	6.566	0.0068 **
Residuals	19	11.20	0.59		

Shapiro-Wilk normality test on above RB-ANOVA residuals:

W	*p*
0.9681	0.5517

Fig S4: Treatment-by-date field soil temperature at 5 cm depth

Tukey's Honest Significant Difference Test of above RB-ANOVA factors:

Temperature (discrete)	*Difference*	*Lower*	*Upper*	*p adjusted*
low-high	-2.871912	-3.528099	-2.215725	0
Treatment				
Double Litter – Control	1.330616	0.4109428	2.2502887	0.0043678 **
No Input – Control	-1.135408	-2.0550804	-0.2157346	0.0143420 *
No Input – Double Litter	-2.466023	-3.3856962	-1.5463504	0.0000048 ***
Block				
B – A	-0.24844749	-1.168120	0.6712254	0.7742015
C – A	-0.09767562	-1.017349	0.8219973	0.9607462
C – B	0.15077186	-0.768901	1.0704448	0.9092669
Temperature : Treatment				
low:C-high:C	-2.7848085	-4.5005676	-1.0690495	0.0007320 ***
high:DL-high:C	1.8372892	0.4363777	3.2382006	0.0062491 **
low:DL-high:C	-2.4675397	-4.1832988	-0.7517806	0.0026108 **
high:NI-high:C	-1.5549771	-2.9558885	-0.1540657	0.0244592 *
low:NI-high:C	-3.0810769	-4.7968360	-1.3653178	0.0002273 ***
high:DL-low:C	4.6220977	2.9063386	6.3378568	0.0000009 ***
low:DL-low:C	0.3172689	-1.6639191	2.2984568	0.9953159
high:NI-low:C	1.2298314	-0.4859277	2.9455905	0.2556817
low:NI-low:C	-0.2962684	-2.2774563	1.6849196	0.9965995
low:DL-high:DL	-4.3048288	-6.0205879	-2.5890697	0.0000026 ***
high:NI-high:DL	-3.3922663	-4.7931777	-1.9913549	0.0000043 ***
low:NI-high:DL	-4.9183661	-6.6341252	-3.2026070	0.0000003 ***
high:NI-low:DL	0.9125625	-0.8031965	2.6283216	0.5596342
low:NI-low:DL	-0.6135373	-2.5947252	1.3676507	0.9192340
low:NI-high:NI	-1.5260998	-3.2418589	0.1896593	0.0988527 .